

**JUNE 2019**

**M. Sc. in Civil Engineering**

**ABDULLAH TÜRER**

**REPUBLIC OF TURKEY  
GAZIANTEP UNIVERSITY  
GRADUATE SCHOOL OF NATURAL & APPLIED SCIENCES**

**EXPERIMENTAL INVESTIGATION OF IMPACT BEHAVIOUR  
OF TIMBER FORMWORK BEAMS STRENGTHENED WITH  
CFRP STRIPS**

**M. Sc. THESIS  
IN  
CIVIL ENGINEERING**

**ABDULLAH TÜRER**

**JUNE 2019**

**EXPERIMENTAL INVESTIGATION OF IMPACT BEHAVIOUR OF  
TIMBER FORMWORK BEAMS STRENGTHENED WITH CFRP STRIPS**

**M. Sc. Thesis**

**in**

**Civil Engineering**

**Gaziantep University**

**Supervisor**

**Prof. Dr. Abdulkadir ÇEVİK**

**by**

**Abdullah TÜRER**

**June 2019**

© 2019 [Abdullah TÜRER]

REPUBLIC OF TURKEY  
GAZIANTEP UNIVERSITY  
GRADUATE SCHOOL OF NATURAL AND APPLIED SCIENCES  
CIVIL ENGINEERING DEPARTMENT

Name of Thesis: Experimental Investigation of Impact Behaviour of Timber  
Formwork Beams Strengthened with CFRP Strips

Name of the Student: Abdullah TÜRER

Exam Date: 17.06.2019

Approval of the Graduate School of Natural and Applied Sciences

Prof. Dr. Ahmet Necmeddin YAZICI

Director

I certify that this thesis satisfies all the requirements as a thesis for the degree of Master  
of Science.

Prof. Dr. Hanifi ÇANAKCI

Head of Department

I certify that this thesis satisfies all the requirements as a thesis for the degree of Master  
of Science.

Prof. Dr. Abdulkadir ÇEVİK

Supervisor

This is to certify that we have read this thesis and that in our consensus opinion it is  
fully adequate, in scope and quality, as a thesis for degree of Master of Science.

Examining Committee Members:

Signature

Prof. Dr. Abdulkadir ÇEVİK

.....

Prof. Dr. Mustafa ŞAHMARAN

.....

Assist. Prof. Dr. Mehmet Eren GÜLŞAN

.....

**I hereby declare that all information in this document has been obtained and presented in accordance with academic rules and ethical conduct. I also declare that, as required by these rules and conduct, I have fully cited and referenced all material and results that are not original to this work.**

**Abdullah TÜRER**

## **ABSTRACT**

### **EXPERIMENTAL INVESTIGATION OF IMPACT BEHAVIOUR OF TIMBER FORMWORK BEAMS STRENGTHENED WITH CFRP STRIPS**

**TÜRER, Abdullah**

**M.Sc. in Civil Engineering**

**Supervisor: Prof. Dr. Abdulkadir ÇEVİK**

**June 2019**

**57 pages**

The formwork systems used in the construction of buildings together with the developing construction technologies have also changed and improved significantly. Especially in the production of high-rise buildings, formwork systems which can be installed quickly, durable to external loads, used more than once, have become a necessity. In the formation of such formwork systems, timber and composite timber are preferred for reasons such as durability, ease of installation, lightness compared to steel systems and easy to use multiple times. The most commonly used structural component in forming such formwork systems are formwork beams and these beams may be damaged due to various reasons during their lifetime. Within the scope of this study, H20 top P type timber formwork beams with 1800 and 2450 mm length which is among the products of DOKA<sup>(c)</sup> company is damaged under the effect of static loading up to a high load level of 85% of the maximum carrying capacity and after being retrofitted using anchored CFRP strips, performance and behavior of the beams under the influence of various loading types such as static, fatigue and impact are investigated experimentally. Two different lengths of retrofitted timber formwork beams were tested by applying monotonic static, fatigue and impact loading and comments were made about the effects of the retrofit method on performance under different loading types.

**Key Words:** Damaged Formwork Beam, Monotonous Static Load, Impact Load, Fatigue Load

## ÖZET

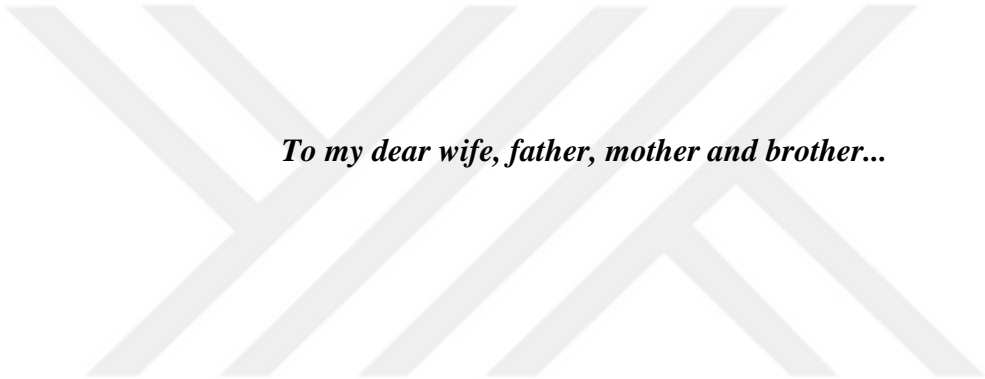
### KARABON TAKVİYELİ ELYAF ŞERİTLER İLE GÜÇLENDİRİLMİŞ AHŞAP KALIP KİRİŞLERİNİN ÇARPIŞMA YÜKLEMESİ ETKİSİNDEKİ DAVRANIŞININ DENEYSEL OLARAK İNCELENMESİ

**TÜRER, Abdullah**

**Yüksek Lisans Tezi, İnşaat Mühendisliği**  
**Tez Yöneticisi: Prof. Dr. Abdulkadir ÇEVİK**  
**Haziran 2019**  
**57 sayfa**

Gelişen inşaat teknolojileri ile birlikte yapıların imalatlarında kullanılan kalıp sistemleri de önemli oranda değişim göstermiş ve gelişmiştir. Özellikle yüksek katlı yapıların imalatlarında çabuk kurulabilen, dış yüklere karşı dayanıklı, birden fazla kere kullanılabilen, kalıp sistemleri gereklilik haline gelmiştir. Bu tür kalıp sistemlerinin oluşturulmasında ahşap ve kompozit ahşap malzemesi, dayanıklılığı, montaj kolaylığı, çelik sistemlere göre hafif olması ve birden fazla kere kullanımının kolay olması gibi nedenlerden dolayı tercih edilmektedir. Bu tür kalıp sistemlerinin oluşturulmasında en fazla kullanılan yapısal bileşen kalıp kirişleri olup, bu kirişler kullanım süreleri içerisinde değişik nedenlerden dolayı hasar görebilmektedir. Bu çalışma kapsamında DOKA<sup>(c)</sup> firmasının ürünleri arasında yer alan H20 top P türünde, 1800 ve 2450 mm uzunluğunda ahşap kalıp kirişlerine maksimum taşıma güçlerinin 85%'i gibi yüksek bir yük düzeyine kadar statik yükleme etkisi altında hasar verdirilmiş ve ankrajlı CFRP şeritler kullanılarak onarıldıktan sonra kirişler statik, yorulma ve ani dinamik çarpma gibi değişik yükleme türleri etkisi altındaki performans ve davranışları deneysel olarak incelenmiştir. İki farklı uzunluktaki onarılmış ahşap kalıp kiriş deney elemanları monotonik statik, tekrarlı yorulma ve ani dinamik çarpma yüklemeleri uygulanarak test edilmiş ve uygulanan onarım yönteminin değişik yükleme türleri etkisindeki performans üzerindeki etkileri hakkında yorumlar yapılmıştır.

**Anahtar Kelimeler:** Hasarlı Kalıp Kiriş, Monotonik Statik Yükleme, Çarpışma Testi, Yorulma Testi



*To my dear wife, father, mother and brother...*

## ACKNOWLEDGEMENTS

During the course of this study, I offer endless gratitude and thanks to my advisor from Gaziantep University faculty members Prof. Dr. Abdulkadir ÇEVİK whose provide full support, share all of knowledge with me, make great efforts in my thesis and who also adds a lot to me as a personality.

In addition, I would like to thank to dear Prof. Dr. Özgür ANIL whose share valuable information with me, never refrain their interests, assists carried out of experiments and laboratory facilities and giving very big supports in thesis writing at every stage of this study.

I am thankful and appreciate my dear friends Res. Asst. Dr. Tolga YILMAZ, Res. Asst. Ömer MERCİMEK and Rahim GHORUBİ who didn't spare me their support in In carrying out experimental works.

I would like to thank my all my family and to my dear wife Semâhat who love, support and trust me during the thesis study.

## TABLE OF CONTENTS

	<b>Page</b>
<b>ABSTRACT</b> .....	iii
<b>ÖZET</b> .....	iv
<b>ACKNOWLEDGEMENTS</b> .....	viii
<b>TABLE OF CONTENTS</b> .....	ix
<b>LIST OF FIGURES</b> .....	xi
<b>LIST OF TABLES</b> .....	xiii
<b>CHAPTER 1</b> .....	1
1.1    General .....	1
1.2    Purpose of Thesis .....	2
1.3    Layout of Thesis.....	3
<b>CHAPTER 2</b> .....	1
<b>LITERATURE REVIEW</b> .....	1
2.1    General .....	1
2.2    Timber Beams Strengthened with CFRP Strips.....	1
2.3    Impact Loading of Timber Beams.....	4
2.4    Fatigue Loading of Timber Beams.....	7
<b>CHAPTER 3</b> .....	11
<b>EXPERIMENTAL PROGRAM</b> .....	11
3.1    Materials.....	11
3.1.1    Wood.....	11
3.1.2    Carbon Fiber Reinforced Polymer (CFRP).....	12
3.1.3    Epoxy Resin .....	12
3.2    Timber Formwork Beam (DOKA H20 top P).....	13

3.3	Test Specimens.....	16
3.4	Test Procedure.....	18
3.4.1	Static and Fatigue Loding .....	18
3.4.2	Impact Loading Test .....	21
3.4.3	Damage Process and Retrofitting with CFRP Strips and Anchor.....	30
<b>CHAPTER 4</b>	.....	<b>34</b>
<b>EXPERIMENTAL RESULTS AND DISCUSSIONS</b>	.....	<b>34</b>
4.1	Static Loading Results.....	34
4.2	Fatigue Loading Results.....	38
4.3	Impact Loading Results.....	42
<b>CHAPTER 5</b>	.....	<b>53</b>
<b>CONCLUSION</b>	.....	<b>53</b>
<b>REFERENCES</b>	.....	<b>56</b>

## LIST OF FIGURES

	<b>Page</b>
<b>Figure 2.1</b> Load versus mid-span deflection for un-strengthened control beams [2] .	2
<b>Figure 2.2</b> Load versus mid-span deflection for strengthened control beams [2].....	2
<b>Figure 2.3</b> (a) Meshed beam with boundary condition (b) Strain contour [7] .....	4
<b>Figure 2.4</b> Schematic drawing of impact test set-up [9] .....	5
<b>Figure 2.5</b> Results of Impact Loading Tests of Timber Beams by Jansson [9] .....	5
<b>Figure 2.6</b> Static versus Impact Strength Results [10].....	6
<b>Figure 2.7</b> Impact Fracture of Wood [11] .....	6
<b>Figure 2.8</b> Load vs. Time Curve [11].....	6
<b>Figure 2.9</b> Oscillatory Load [16].....	8
<b>Figure 2.10</b> Behaviour for a Load Cycle [16] .....	9
<b>Figure 2.11</b> Moment-rotation hysteretic curve of the specimen CJ1 and CJ3 [17] ...	9
<b>Figure 2.12</b> Envelope curve of the specimen under cyclic loading [17].....	10
<b>Figure 3.1</b> Borgund church, Norway, twelfth century [18].....	11
<b>Figure 3.2</b> Dimensions of H20 P Beam and Cross-section.....	13
<b>Figure 3.3</b> Deflection Diagram of the H20 P Beam [21] .....	13
<b>Figure 3.4</b> DOKA H20 top P Timber Formwork Beam.....	14
<b>Figure 3.5</b> Constructional Use of DOKA Beams .....	15
<b>Figure 3.6</b> Dimensions and Retrofitting Details of Test Specimens .....	17
<b>Figure 3.7</b> Test setup for monotonous static and high load level fatigue load.....	19
<b>Figure 3.8</b> During the Static Loading of Retrofitted Beam (Specimen 1) .....	20
<b>Figure 3.9</b> During the Fatigue Loading of Retrofitted Beam (Specimen 7) .....	21
<b>Figure 3.10</b> Impact responses of a RC member [22] .....	22
<b>Figure 3.11</b> Free weight drop test setup for impact load.....	23
<b>Figure 3.12</b> Load cell with model number 200C50 produced by PCB Group.....	24
<b>Figure 3.13</b> Mounting of the load cell on the impact test .....	24
<b>Figure 3.14</b> Piezoelectric Accelerometer PCB Group ICP 352B70 Model .....	25
<b>Figure 3.15</b> Correct mount methods of piezoelectric accelerometers [23] .....	25
<b>Figure 3.16</b> Mounting of piezoelectric accelerometer on test specimens .....	26

<b>Figure 3.17</b> LPS100 Model Linear Potentiometer of Opkon Company (LVDT).....	26
<b>Figure 3.18</b> Installation of Linear Potentiometer (LVDT).....	27
<b>Figure 3.19</b> (a) NI 9234 (b) NI 9235 (c) NI 9201 .....	27
<b>Figure 3.20</b> Failure Mode of Specimen 3.....	28
<b>Figure 3.21</b> Failure Mode of Specimen 4.....	28
<b>Figure 3.22</b> Failure Mode of Specimen 5.....	28
<b>Figure 3.23</b> Failure Mode of Specimen 8.....	29
<b>Figure 3.24</b> Failure Mode of Specimen 9.....	29
<b>Figure 3.25</b> Failure Mode of Specimen 10.....	29
<b>Figure 3.26</b> Damage Limit of 1.80 m Timber Beam.....	30
<b>Figure 3.27</b> Damage Limit of 2.45 m Timber Beam.....	30
<b>Figure 3.28</b> Cutting of CFRP Strips.....	31
<b>Figure 3.29</b> (a) CFRP Anchor Diameters (b) CFRP Wrap on Iron Piece ( $\phi 8$ ).....	31
<b>Figure 3.30</b> (a) Making a Hole in Timber (b) Drilled Timber Beams .....	32
<b>Figure 3.31</b> (a) Preparation of Epoxy (b) CFRP Bonding .....	32
<b>Figure 3.32</b> Details of CFRP Fan Type Anchor.....	33
<b>Figure 3.33</b> (a) Finding the Drill Hole (b) CFRP Anchors .....	33
<b>Figure 3.34</b> (a) Fan Type CFRP Application (b) Retrofitting with CFRP.....	33
<b>Figure 4.1</b> tatic Load-Displacement Graphs of Specimens.....	35
<b>Figure 4.2</b> Strain Distribution Graphs of Specimen for Static Loading.....	36
<b>Figure 4.3</b> Calculation Approach of Ultimate Load Capacity, Initial Stiffness, Displacement Ductility Ratios and Energy Dissipation Capacity.....	38
<b>Figure 4.4</b> Displacement Chancing Graphs of Specimens under Fatigue Load .....	40
<b>Figure 4.5</b> Strain Distribution Graphs of Specimen for Fatigue Loading.....	42
<b>Figure 4.6</b> Left Acceleration-Time Graphs of Specimens under Impact Load.....	44
<b>Figure 4.7</b> Displacement-Time Graphs of Specimens under Impact Load.....	45
<b>Figure 4.8</b> Maximum Strain-Time Graphs of Specimens under Impact Load.....	46
<b>Figure 4.9</b> Impact Load-Time Graphs of Specimens .....	47
<b>Figure 4.10</b> CFRP Strain Distribution Graphs of Specimens at Ultimate Load Level under Impact Load .....	48
<b>Figure 4.11</b> Failure Modes of All Specimens .....	52

## LIST OF TABLES

	<b>Page</b>
<b>Table 3.1</b> Mechanical Properties of CFRP [19] .....	12
<b>Table 3.2</b> Mechanical Properties of Epoxy Resin [20] .....	12
<b>Table 3.3</b> Permissible Values of H20 P Beam [23].....	14
<b>Table 3.4</b> Mechanical Properties of Spruce Wood.....	15
<b>Table 3.5</b> Mechanical Properties of Compacted Particle Board .....	15
<b>Table 3.6</b> Properties of Test Specimens .....	16
<b>Table 3.7</b> Fatigue Loading Values of 2.45 m Timber Beam.....	19
<b>Table 3.8</b> Fatigue Loading Values of 1.80 m Timber Beam.....	20
<b>Table 3.9</b> Technical Specifications for the Data Logger NI 9234.....	28
<b>Table 4.1</b> Experimental Result for Static Loading Test .....	34
<b>Table 4.2</b> Experimental Result for Fatigue Loading Test .....	41
<b>Table 4.3</b> Experimental Result for Impact Loading Test .....	50

## CHAPTER 1

### INTRODUCTION

#### 1.1 General

Timber is a material with high thermal and acoustic insulation properties. It has been used for centuries due to its high strength/weight ratio as well as its aesthetic properties, easy processing, fiber structure, excellent thermal and sound insulation and better durability properties compared to other materials used as building materials [1].

Wood; there is a certain carrying capacity even though it is not as high in strength as concrete or steel in proportion to weight. It may be preferred because it is light compared to other structural members. There are also many areas where the wood was used together with the steel. Nowadays wood is not used too much as structural member in Turkey even though it is used as an international field, especially in USA. Even, the tallest wooden building in the world, the Brock Commons, 53 meters high at the University of British Columbia, is used as a student residence. Wood is used as a formwork element for reinforced concrete structures and other purposes rather than structural members in most countries. Formwork systems used in the manufacture of large-scale reinforced concrete structures with high-rise or very large construction area have become a necessity to provide features such as being modular, easy to install, economical and having high strength in order to shorten the construction period and to ensure better quality production. Timber beams examined in this thesis are generally used as formwork material in Turkey. For the healthy progress of the construction these formwork materials have to be resistant and durable. In addition, there has been a need for retrofitting of ancient timber structures that have been damaged for various reasons or have changed their intended use. Research on the strengthening and retrofitting of timber or composite timber beams with steel and various composite materials has been found in the literature. However, it has not been found a study that examined the behavior and performances of the different types of load by retrofitting

with anchored CFRP strips after loading and damaging them to a high load level of 85% of the carrying capacity of special timber formwork beams produced as a prefabricated product in the literature review. Therefore, an experimental study was carried out and CFRP material was chosen as the retrofit material. CFRP material is a preferred material in such repair applications because it does not change the geometric dimensions and weight of the structural element in which it is used, also preferred due to its lightness, resistance to environmental influences and high resistance. Within the scope of this study, H20 top P type timber formwork beams, which are among the products of DOKA ©, which is designing this kind of formwork systems using timber materials, have been loaded up to a high load level such as 85% of the carrying capacity and the beams are damaged. Afterwards, damaged timber formwork beams were repaired with CFRP fan type anchored CFRP strips and their behavior under the influence of monotonic static, fatigue and impact loads were investigated. Damaged and retrofitted 2 different sized timber formwork beams with 1800 mm and 2450 mm length were tested under the effect of monotonically increasing static loading, high loading low cycle fatigue and impact loading at 3 different energy levels at scope of work. General load-displacement behaviors, initial stiffnesses, displacement ductility rates, energy dissipation capacities and collapse mechanisms under the effect of static loading of test specimens, change in displacement capacities under the effect of fatigue loading and collapse mechanisms, acceleration-time, displacement-time, multiplication loading-time, maximum strain-time behaviors under the effect of impact loading have been examined and interpreted as a result of tests of retrofitted damaged timber beam test specimens.

## **1.2 Purpose of Thesis**

Timber and composite timber materials are preferred due to their durability, ease of installation, lightness compared to steel systems and easy to use more than one time. It is aimed to investigate the behavior of retrofitted damaged timber formwork beams under the effect of static, fatigue and impact loads, which are used in reinforced concrete structure construction at high and medium height specially produced for this purpose in timber formwork systems. Also, the fact that no such study has been found in the literature is among the aims of this issue.

The greatest effect of timber formwork beams is the impact effect. This is caused by the formwork falling from the top, accidental dropping of any heavy object, explosions and vehicle crashes etc. Therefore, this thesis mostly aims to investigate the impact of timber formwork beams under the different energetic collision loads. In addition to the impact behavior, monotonic static and fatigue behavior of retrofitted damaged timber beams were examined.

### **1.3 Layout of Thesis**

This thesis study is separated into 5 different chapters as follow.

Chapter 1 is an introduction part of the thesis and it contains a brief information and includes a preamble mentioning about the purpose of the thesis.

Chapter 2 is a literature review section on static loading, fatigue loading, impact loading and strengthening with CFRP strips which we performed in this thesis. In addition, literature review of different types of test specimens like concrete made with these loading types is also included.

Chapter 3 is the core section of the thesis and includes materials used in experiments and their properties, test specimen properties and dimensions, test setups, static, fatigue and impact loading procedures and measuring instruments used in these loading tests and some specimen photos after the experiments.

In Chapter 4, the experimental results are examined in detail and shown in the graphs. All results are given in tabular form. Also, the results of each test specimen were interpreted in detail.

Chapter 5 is conclusion part of the thesis and include the failure mechanism of the test specimens under the effect of 3 different loading types. Finally, data from the test results are examined, interpreted and listed.

## **CHAPTER 2**

### **LITERATURE REVIEW**

#### **2.1 General**

Timber beams are preferred for years because they are easy to use, lightweight and durable construction elements. For this reason, researchers are interested in those materials. Although there are many studies on the wood and timber, there is almost no work on the timber formwork beams.

In this section, studies on timber beams will be investigated in various ways. In addition, strengthening with CFRP strips studies also included. The literature review section consists of Impact Loading of Timber Beams, Fatigue Loading of Timber Beams and Timber Beams Strengthened with CFRP Strips sections. Each section will be discussed and evaluated individually with relevant articles.

#### **2.2 Timber Beams Strengthened with CFRP Strips**

Khelifa and Celzard did a numerical analysis of flexural strengthening of timber beams reinforced with CFRP strips. They analyzed strengthened beams using standard FE program. Also, they observed that the CFRP strips increased the load carrying capacity. The results of the analyzes were compared with experimental studies and it was found that the proposed formulation can efficiently capture the global response with acceptable accuracy [2].

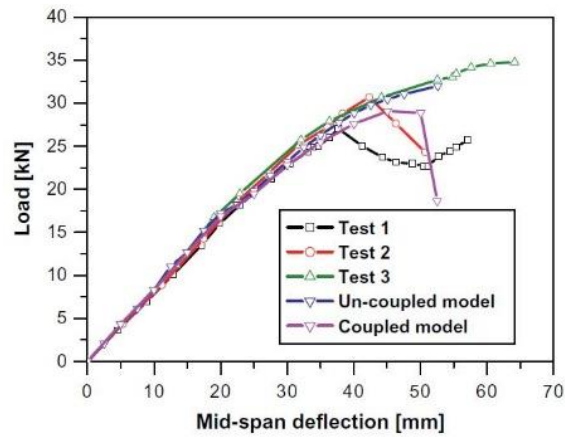


**Figure 2.1** Load versus mid-span deflection for un-strengthened control beams [2]

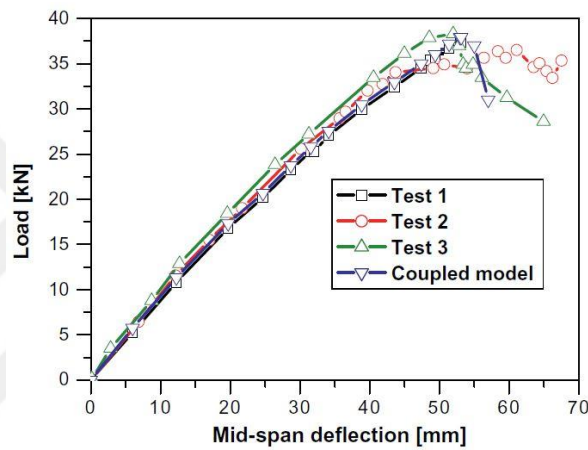


**Figure 2.2** Load versus mid-span deflection for strengthened control beams [2]

Figure 2.1 and 2.2 shows comparison between simulation and experiment results.

Subhani, Globa, Al-Ameri and Moloney studied the flexural strengthening of LVL beam using CFRP. In this study, A comparison is made of type of the CFRP strips are bonded on LVL beam. While the U-wrap shape increases the load carrying capacity by an average of 25%, only the CFRP strip bonded to the beam tension surface has increased by 10%. Finally, it is stated that both applications give successful results in terms of carrying capacity [3].

Schober and Rautenstrauch made experimental investigations on flexural strengthening of timber structures with CFRP in 2005. CFRP strengthening was carried out in different regions of the wood sample and the results were evaluated.

CFRP strengthening was carried out in different locations of the timber sample and the results were evaluated. In this study, two types of strengthening were carried out: internal reinforcement and external reinforcement. In this experiment, The carrying capacity of the timber beams varied between 35 and 87 kN and it was observed that the beam did not carry the load after the first break [4].

D'Ambrisi, Focacci and Luciano investigated the flexural behavior of timber beams repaired with CFRP plates. They used six new timber beams and six old timber beams taken from the floor of an ancient historical building were tested. Two new beam and other old beams were retrofitted with CFRP. Others, strengthened with CFRP strips and tested. As a result of this study, it has been seen that CFRP strips are very effective for both old beams and new beams and increase the carrying capacity significantly [5]. As seen in their work CFRP plates are also used for repair and retrofit purposes.

Researchers Li, Xie and Tsai presented improvement of the flexural performance of retrofitted timber beams using CFRP strips. The main purpose of this study is to investigate the carrying capacity of wooden beams retrofitted with CFRP strips. Firstly, a theoretical analysis of timber beams retrofitted with CFRP composite sheets was obtained and then four-point bending test was used to determine the load–displacement relationships of the timber beams. In this study, it was observed that the mid-point displacement of the beam decreased and the flexural strength of the beam increased with CFRP strip application compared to those without CFRP strip [6].

Kim and Harries present a numerical three-dimensional finite element analysis (FEA) model to examining the behavior of timber beams strengthened with CFRP strips based on the orthotropic characteristics of timber. In this study, it was observed that strengthening with CFRP strips increased the carrying capacity for all Northern White Cedar, Douglas Fir, Sitka Spruce, Yellow Birch and Yellow Poplar species using the mechanical properties of those timber beams [7].

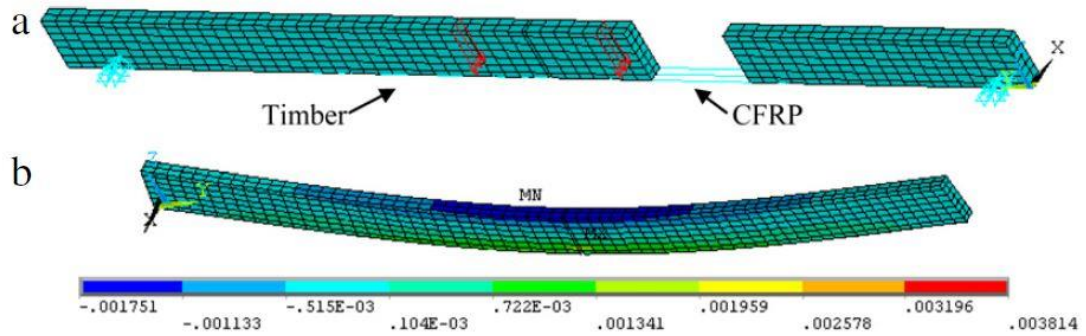


**Figure 2.3** Model: (a) Meshed beam with boundary condition (b) Strain contour [7]

Borri, Corradi and Grazini conducted a study on the reinforcement of existing wood elements under bending loads using CFRP materials. An analytical investigation was first conducted on the behavior of a generic CFRP-reinforced wood section. Then, an experimental study based on a four-point bending test configuration is proposed to characterize the ductility, stiffness and strength response of FRP-timber beams. Mechanical tests on strengthened timber beams showed that the bonding of FRP material to the external surface increased its flexural capacity and stiffness. After all, the use of CFRP can be applied as a strengthening technique without necessitating the removal of the overhanging portion of the structure. The technique used proved to be easy and fast to execute, even when on in situ parts. Especially, it demonstrated to be very promising in many cases of reinforcement of old, historical structural wood parts [8].

### 2.3 Impact Loading of Timber Beams

There is not much research in this area, so I decided to make the thesis topic in this subject. Although there are studies of reinforced concrete under impact loading, the work of timber impact loading is very low.

One of the earliest study on impact loading of timber beams is Bength Jansson's master thesis work in 1982 [9]. The test setup is given in Figure 2.4 and the results are given in Figure 2.5 in his thesis work.

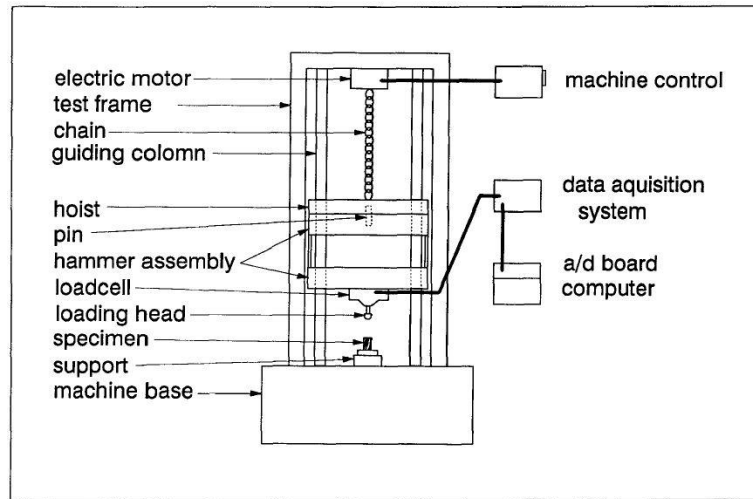


**Figure 2.4** Schematic drawing of impact test set-up [9]

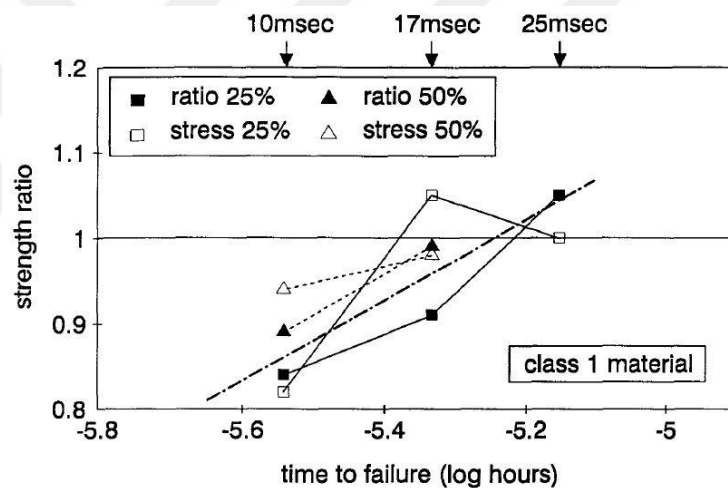


**Figure 2.5** Results of Impact Loading Tests of Timber Beams by Jansson [9]

Leijten investigated the Impact crash and simulation of timber beam. Tests were carried out on three selected wood species and three temperature treated wood species. Three points impact bending tests were performed with a loading speed of 7m/s. Peculiar impulse transmitting effect were detected by the high-speed camera (9000 images/s). It was concluded that the impact behaviour is wood species and grade dependent. Some wood species didn't show any significant bending strength reduction for others the reduction was dramatic [10].

In addition, static and impact test results were compared according to 7 different types of tree in this study by Leijten and shown in the figure 2.6.

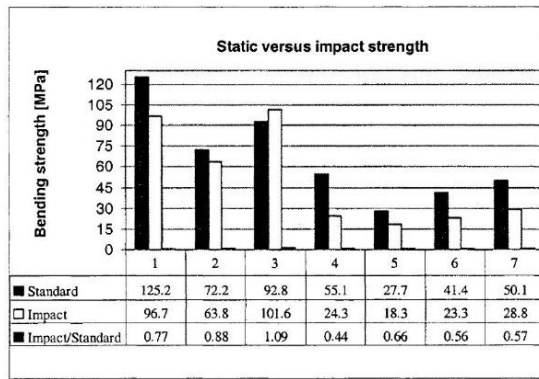


**Figure 2.6** Static versus Impact Strength Results [10]

Mindess and Madsen observed the fracture of wood under impact loading. High speed motion picture photography was used to study the fracture, under impact loading, of wood beams. Photographs were taken at the rate of 500 frames per second, which permitted the crack development during the fracture event to be monitored. Load vs. time data during the test were also recorded. This work presents a photographic record of the crack patterns which developed when the beams were tested in an instrumented impact machine [11].

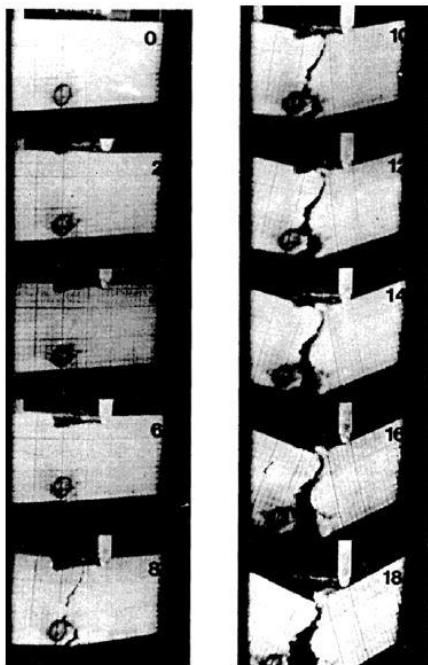


**Figure 2.7** Impact Fracture of Wood [11]

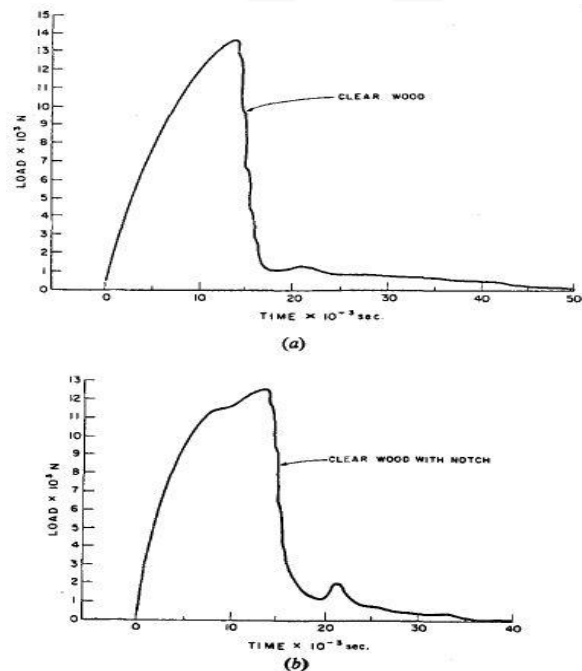


**Figure 2.8** Load vs. Time Curve [11]

Bocchio, Ronca and Van de Kuilen studied impact loading tests on timber beams. They compared the static and impact bending strength two species, Angelim vermelho (*Dinizia excelsa*) and Douglas fir (*Pseudotsuga menziessi*) have been investigated. The hammer consists of a mass of 196 KG in such a shape that the centre of gravity is below the centre of gravity of the timber beam to be hit by the mass. Beams tested as simple supported beams over a span of 1400 mm and drop height of 2540 mm. Considering uniformly accelerated motion, the impact velocity is  $v = 7.06$  m/s and the period of falling of the mass is 0.72 s. The corresponding impact energy is 4.88 kJ. In conclusion, the two species behave in different ways: the average value of the impact strength  $f_d$  for Angelim is higher than the average value  $f_s$  the static strength  $f_s$ , while for Douglas they are almost the same [12].

#### **2.4 Fatigue Loading of Timber Beams**

Madhoushi and Ansell carried out an experimental study on behaviour of timber connections using glued-in GFRP rods under fatigue loading. They described the static and fatigue behavior of in-line beam to beam connections made using glass fibre-reinforced plastic (GFRP), pultruded rods bonded into the end grain of LVL beams with epoxy resin in this study. The results show that solid LVL beams have significantly higher static and fatigue strengths than beams jointed using GFRP glued-in rods, but the capacity of solid LVL to dissipate energy under cyclic loading is much less than for the jointed beams [13].

Yeoh, Fragiaco and Carradine studied the Fatigue behaviour of timber–concrete composite connections and floor beams. The researchers carried out a research on the timber-concrete composite system in this study. The main advantage is that the compressive strength of concrete is exploited through the use of composite action while timber beams are able to resist the tensile stresses. This composite system, which is usually used in bridges, is subjected to cyclic loading. Fatigue behaviour of two types of timber–concrete connection investigated were: (i) a rectangular notch connection reinforced with a coach screw (also known as lag screw); and (ii) a connection with toothed metal plates punched into laminated veneer lumber (LVL). Although the rectangular notch connection was stand on 2 million cycles, the metal plate connection was failed after 350.000 cycles. In this respect, the rectangular notch

connection system is recommended for use in bridge design as opposed to metal plate connections [14].

Tsai and Ansell experimentally studied the fatigue properties of wood in flexure. Different types of laminates were fatigue tested under load control in four point flexure. Tests were conducted in repeated and reversed loading over a range of five  $R$  ratios at three moisture contents. Increased moisture content reduces the static strength and fatigue life and reversed loading results in the lowest fatigue life. In conclusion, Fatigue life is largely species independent when normalized by its static strength. This is similar to the normalizing effect density has on static strengths. Only where the wood structure is significantly changed as for the compressed beech laminates are fatigue lives affected [15].

American researchers Balogh and Atadero made an experimental study of fatigue testing of Wood-Concrete composite beams. They worked on wooden concrete composite elements and embedded the anchor with. Also, an example of the oscillation graph is given in Figure 2.9 and behavior of a load cycle given in figure 2.10 [18].

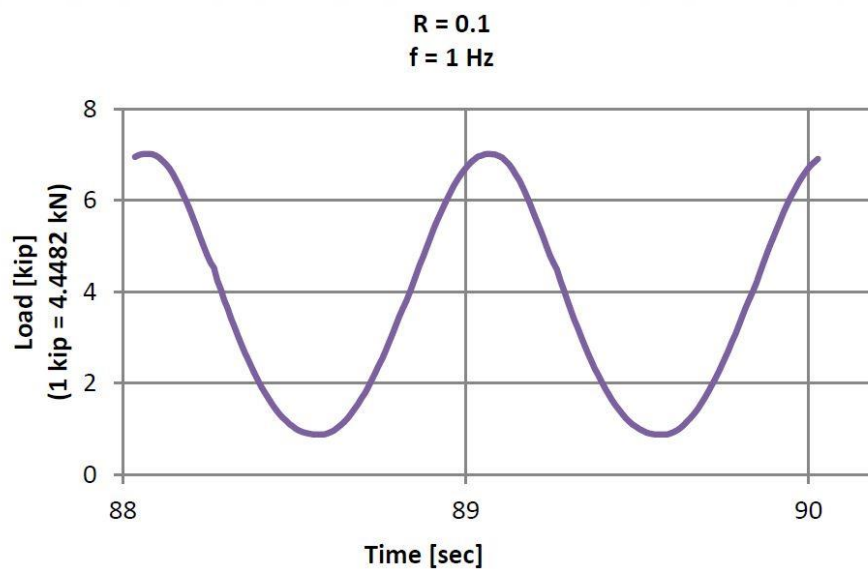


**Figure 2.9** Oscillatory Load [16]

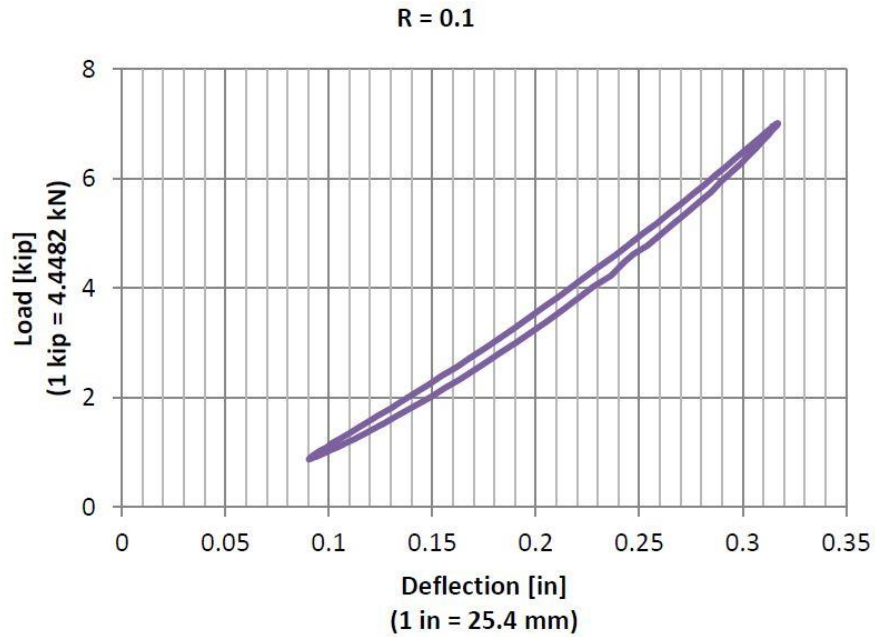


**Figure 2.10** Behaviour for a Load Cycle [16]

Zhou, Huang, Ni, Shen and Zhao made an experiment on bamboo (Timber) frame structure under fatigue loading. The specimens were loaded under displacement control with a rate of 10 mm per minute until the specimens reach failure. In this study, failures of 3 test specimens were caused by the buckling of flanges in the compression and that the steel of connections does not yield. Also, curves related this topic given in figure 2.11, 2.12 and 2.13 [17].

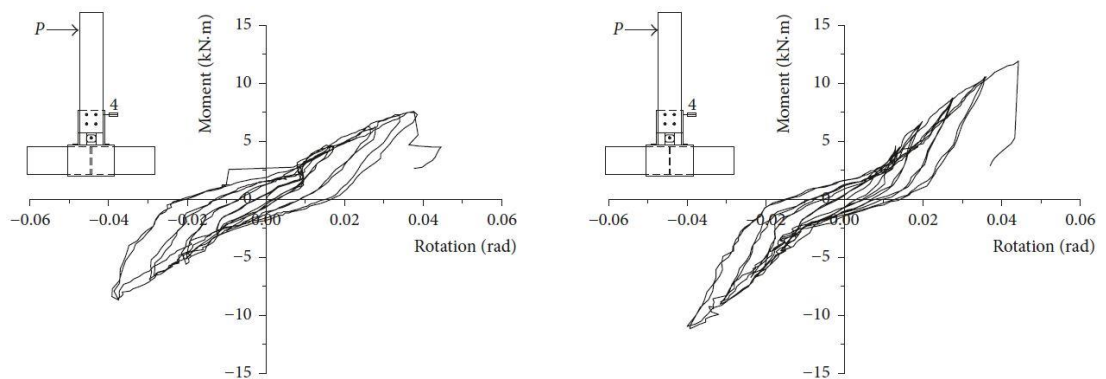


**Figure 2.11** Moment-rotation hysteretic curve of the specimen CJ1 and CJ3 [17]

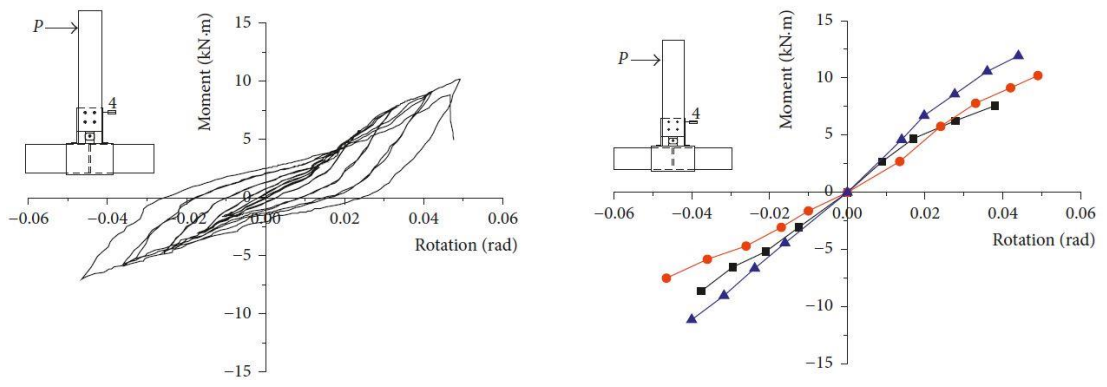


**Figure 2.12:** Envelope curve of the specimen under cyclic loading (Right Side) [17]



## CHAPTER 3

### EXPERIMENTAL PROGRAM

#### 3.1 Materials

The most important part of the thesis work is the selection of the materials to be used. The material type and quality are also important after the materials to be used are selected. In this thesis, wood, Carbon Fiber Reinforced Polymer (CFRP) and epoxy adhesive are used.

##### 3.1.1 Wood

Wood material is biologically 'produced' in the growing tree to meet the needs of the tree itself. In this respect, it is a high quality fiber composite, optimally designed to resist loads acting on the tree, but also to provide transport of water and nutritional agents [18].

Wood is an oldest building material. Protection and shelter against wind, rain and cold is a very basic need for mankind. Since ancient times, wood has been the most important material used for this purpose [18].

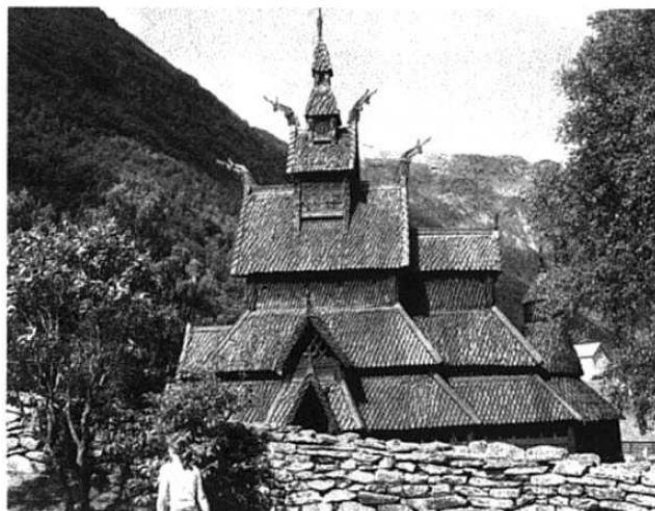


**Figure 3.1** Borgund church, Norway, twelfth century (Photo: Lund University) [18]

Wood which is widely used in ancient times as seen in figure 3.1 is still using as a building material. The spread of reinforced concrete structures has reduced the use of wood. However, because of the cost and lightweight its usage is increasing rapidly combined with steel structure. In addition, the use of concrete as a formwork material is quite common in our country. In this thesis study, DOKA timber formwork beams with increased strength with today's technology have been preferred.

### 3.1.2 Carbon Fiber Reinforced Polymer (CFRP)

CFRP is generally used for rehabilitation due to its high tensile strength in structural elements damaged by various factors. Advantages of strengthening with CFRP have been demonstrated in the literature review and are included in Section 2. In this study, SikaWrap®-230 C Woven Carbon Fiber Fabric for structural strengthening produced by Sika Construction Chemicals Inc. was used. The mechanical properties of CFRP are given in table 3.1.

**Table 3.1** Mechanical Properties of CFRP [19]

<b>Properties of CFRP</b>	<b>Value</b>
Thickness (mm)	0.131
Tensile Strength (MPa)	4300
Modulus of Elasticity (MPa)	238000
Elongation at Break (%)	1.8

### 3.1.3 Epoxy Resin

Sikadur-330 epoxy is used for bonding and strengthening CFRP strips and anchors to wooden samples. Also, the suitable epoxy for SikaWrap®-230 CFRP is Sikadur-330, which is catalyzed by Sika. The mechanical properties of epoxy are given in table 3.2.

**Table 3.2** Mechanical Properties of Epoxy Resin [20]

<b>Properties of Epoxy</b>	<b>Value</b>
Tensile Strength (MPa)	30
Modulus of Elasticity (MPa)	3800

### 3.2 Timber Formwork Beam (DOKA H20 top P)

H20 N timber formwork beams produced by DOKA company in Austria were used in this thesis study. Two types of beams were used in lengths of 180 cm and 245 cm.

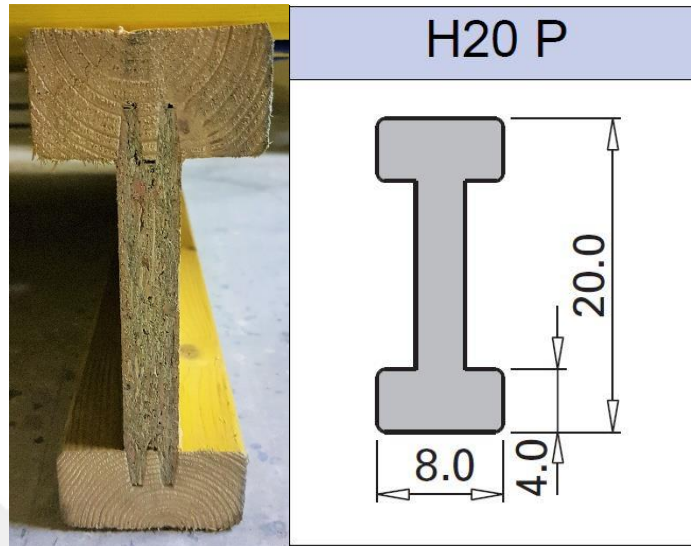


**Figure 3.2** Dimensions of H20 P Beam and Cross-section

The Company cover the ends of the beams with polyurethane material so that they do not get damaged when they fall off the top. It has innovative polyurethane end reinforcement for highly effective protection of the formwork beam. This is an effect that extends the life of the beam. This material gave the extra strength to beam because it was applied thereby melting. Company are assuming 12% timber moisture content.

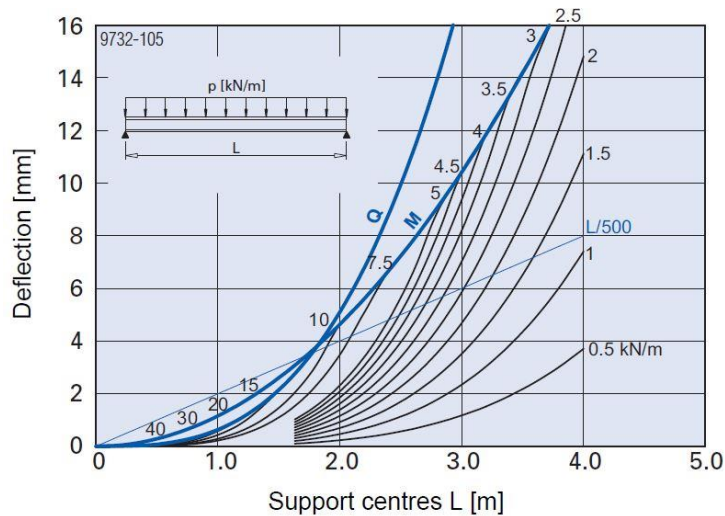


**Figure 3.3** Deflection Diagram of the H20 P Beam [21]

M represents permitted bending moment, Q represents permitted shear force and P represents actual load in figure 3.3. Also, the values allowed in the DOKA's catalog are given in Table 3.3 below.

**Table 3.3** Permissible Values of H20 P Beam [23]

	H20 P Value
Perm. Q [kN]	11
Perm. M [kNm]	5
E.J [kNm <sup>2</sup> ]	450
Perm. Span [m]	4

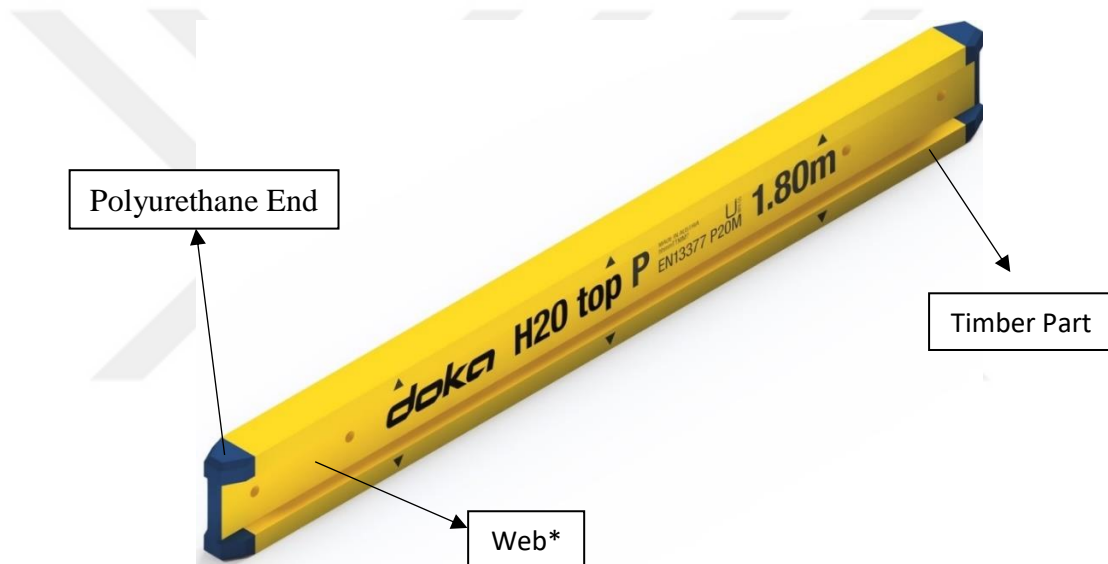


**Figure 3.4** DOKA H20 top P Timber Formwork Beam

\* Web part made of wood and wood-based materials. It is special flat compressed particle board. Thickness of web is 22.0 mm. Section of web is given in figure 3.2.



**Figure 3.5** Constructional Use of DOKA Beams

Mechanical properties of spruce materials using for I beam flanges and compacted particle board using for I beam web are given in Table 3.4 and Table 3.5, respectively.

**Table 3.4** Mechanical Properties of Spruce Wood

<b>Properties</b>	<b>Value</b>
Compressive strength parallel to grain	38.7 MPa
Compressive strength perpendicular to grain	4.0 MPa
Tensile strength parallel to grain	75.8 MPa
Tensile strength perpendicular to grain	2.6 MPa
Shear strength parallel to grain	7.9 MPa
Elastic Modulus	10.8 GPa
Poisson Ratio	0.467

**Table 3.5:** Mechanical Properties of Compacted Particle Board

<b>Properties</b>	<b>Value</b>
Compression strength	13.75 MPa
Tension strength	8.6 MPa
Shear strength	8.6 MPa
Elastic Modulus	6.55 GPa
Poisson Ratio	1.022

### 3.3 Test Specimens

H20 top P type formwork beam, which is among the products of Doka<sup>®</sup>, was chosen as the test specimen for testing. Within the scope of the study, firstly, the timber formwork beams were damaged by a 3-point bending test in monotonic static loading effect up to 85% of their maximum carrying capacity. Then, the damaged timber formwork beams were retrofitted with CFRP fan type anchored CFRP strips and three different types of loading were tested until they were failed and their behavior was interpreted. The formwork beams tested in the experimental study were selected as 2 different lengths of 1800 mm and 2450 mm and their geometrical dimensions are given in Figure 3.6. Timber formwork beam H20 top P is a solid-web beam in accordance with EN 13377 with innovative polyurethane end reinforcement for increased resistance to mechanical stresses and strains. Solid-web beam made of wood and wood-based materials to EN 13377. Wood for the flanges is spruce. Web of the H20 type P is made from compressed particle board. Surfaces of the timber beams are painted yellow varnish without wood preservatives. The variables examined within the scope of the experimental study are the span of the timber formwork beams and the type of loading on the beams. The properties of the test specimens included in the experimental program are presented in Table 3.6.

**Table 3.6** Properties of Test Specimens

Spec. No.	Loading Type	Beam Span (mm)	Drop Height (mm)	Hammer Weight (kg)
1	Monotonic static	1800	-----	-----
2	Fatigue		-----	-----
3	Impact		500	84
4			750	
5			1000	
6	Monotonic static	2450	-----	-----
7	Fatigue		-----	-----
8	Impact		500	84
9			750	
10			1000	

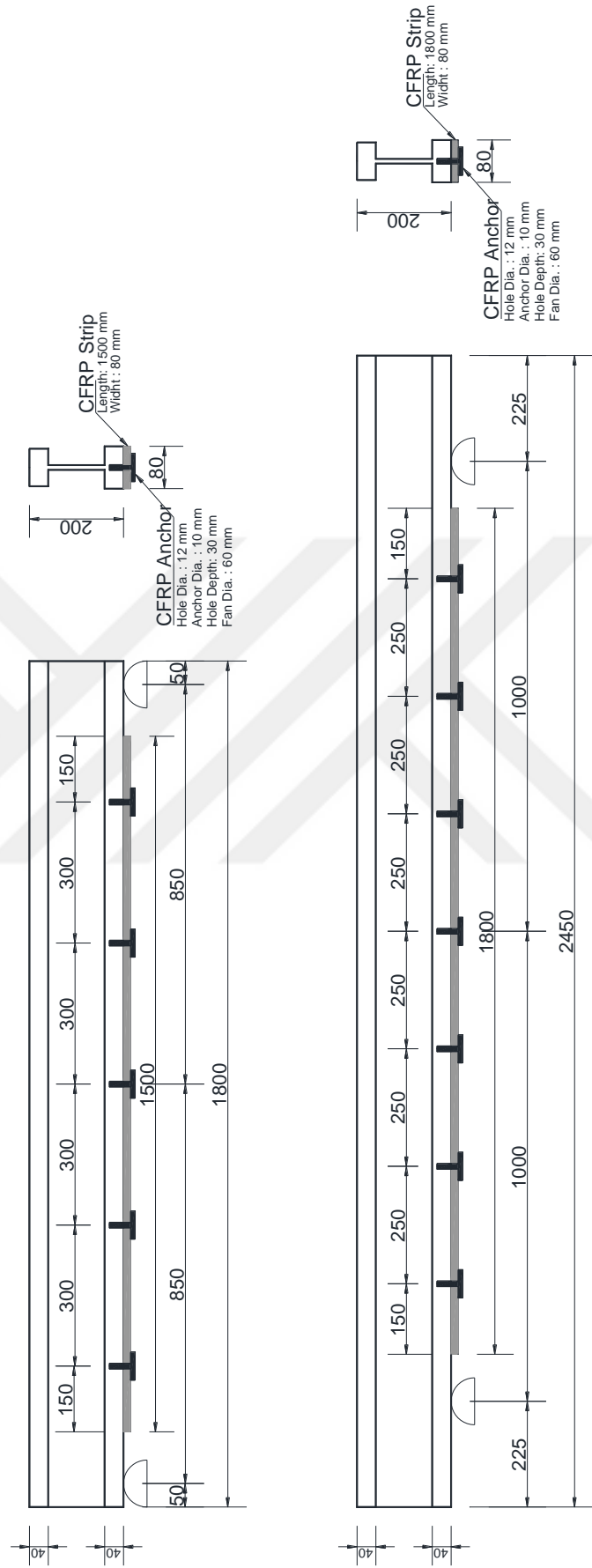


**Figure 3.6** Dimensions and Retrofitting Details of Test Specimens

### **3.4 Test Procedure**

#### **3.4.1 Static and Fatigue Loading**

The 3-point bending load is applied to the experimental specimens in all three loading types to the full center opening of the timber beams with the axis of symmetry. In the experimental study, monotonically increased static loading and high load level fatigue loading tests were performed in the MTS 322 model, a 500 kN servo-hydraulic loading system. The speed of the monotonically increased static load applied to the test specimens was applied to the timber beam test specimens of both lengths to be equal to 0.5 mm/sec. Experiments were carried out by drawing the load-displacement graphs during the tests by measuring the beam displacement at the center of the beam where the loading is applied from the test specimens and measuring the applied load and strain values measured from 6 points on the CFRP strip glued to the beam tension surface for repair. The loading was applied by using the servo-hydraulic actuator of the 500 kN capacity test device, which can be adjusted according to the displacement. MTS, which is used in static loading tests, is given in Figure 3.7. As a result of the static loading, the general load-displacement behaviors and maximum carrying-capacity values of the two different length timber formwork test specimens were determined and this information was used to create the loading profile of the high load level fatigue test which is the second loading type to be examined in the experimental study. The fatigue loading profile, which varies between 85% and 10% of the maximum bearing capacity values, is applied to the test specimens with a frequency of 4 hZ. The ratios of maximum fatigue load and minimum fatigue load values are 8.5 for the beam test specimens of both lengths and the minimum fatigue load is at a level of 12% of the maximum fatigue load. This fatigue loading cycle was applied to the test specimens four times per second. The fatigue loading applied to the test specimens is identical to the static loading applied as a 3-point bending loading and the displacement values of the mid-span of the beam, changes of the applied load and strain values measured from 6 points on the CFRP strip glued to the beam tension surface for repair are measured.

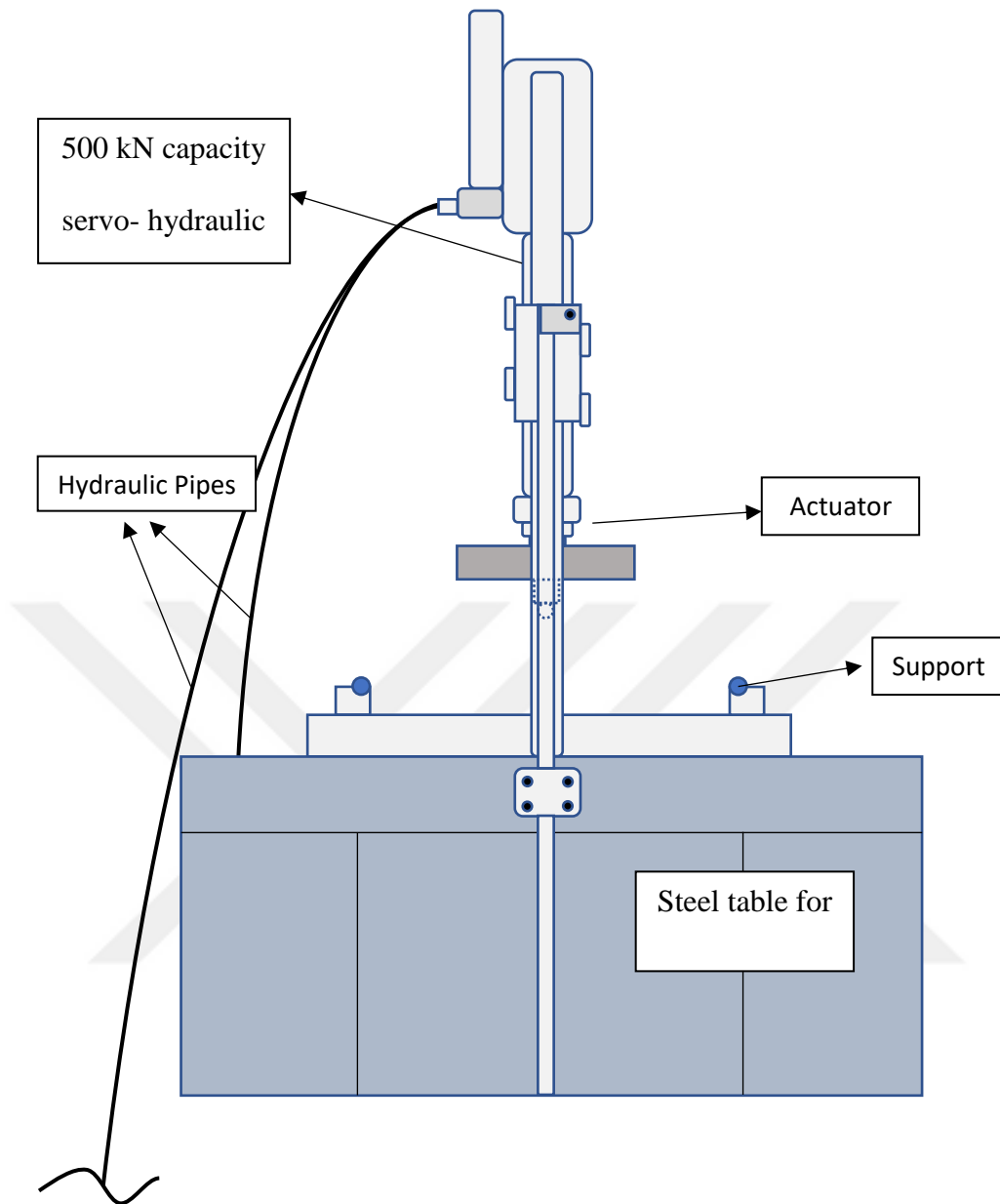


**Figure 3.7** Test setup for monotonous static and high load level fatigue load

The position of the strain gauges taken from the CFRP strips during the test and the static and fatigue loading test setup are given in Figure 3.8 and 3.9, respectively.

**Table 3.7** Fatigue Loading Values of 2.45 m Timber Beam

Name	Value	Unit
Wave Shape	Sine	-
Frequency	2.00	Hz
Absolute End Level 1	-2.61	kN

Absolute End Level 2	-20.00	kN
Preloading Value	-1.00	kN
Time to Complete PL	2.00	sec
# of Data Collection	5.00	Hz

**Table 3.8** Fatigue Loading Values of 1.80 m Timber Beam

Name	Value	Unit
Wave Shape	Sine	-
Frequency	2.00	Hz
Absolute End Level 1	-4.00	kN
Absolute End Level 2	-24.00	kN
Preloading Value	-1.00	kN
Time to Complete PL	2.00	sec
# of Data Collection	5.00	Hz



**Figure 3.8** During the Static Loading of Retrofitted Beam (Specimen 1)



**Figure 3.9** During the Fatigue Loading of Retrofitted Beam (Specimen 7)

### **3.4.2 Impact Loading Test**

The third load type applied in the experimental study, the impact loading design was carried out by the researchers and implemented using a special free weight reduction test setup. This test apparatus is designed to drop the weight from 2500 mm height with a weighing up to 250 kilograms and is a previously used test apparatus in such studies. Within the scope of the study, constant hammer weighing 84 kilograms has been dropped from 3 different 500, 750 and 1000 mm heights and impact loading at 3 different energy levels was applied to the test specimens. The hammer used in the test apparatus has a semi-spherical cap made of high-strength steel. The impact loading applied to the test specimens on the center of the opening, exactly to the axis of symmetry and at this point a 150x100x15 mm size steel loading plate made of high-strength steel is used to effect the impact energy uniformly on the test specimen section. From the timber beam test specimens, strain values measured from 6 points on the CFRP strip glued to the beam tension surface for repair, 2 acceleration measurements from left and right side at a distance of 300 mm from the axis of beam symmetry and 2 mid-span displacement measurements from the left and right sides at a distance of 50 mm were measured. In addition, the impact load applied to the test specimens was also measured with a dynamic load cell connected to the steel hammer.

All measurements were taken using data logger designed specifically for dynamic impact tests, which can take 10 kHz measurements per channel depending on time. The free drop weight test apparatus designed by the graphers used in the experimental study is given in Figure 3.11.

Impact loading tests have been carried out many times on reinforced concrete structural elements, but they have never been done on timber structural elements. For example, the reaction of the reinforced concrete beam to sudden loading is as seen in figure 3.10. While reinforced concrete structure elements tends to deflect more at the end of impact loading, timber structural elements exhibit a more elastic behavior.

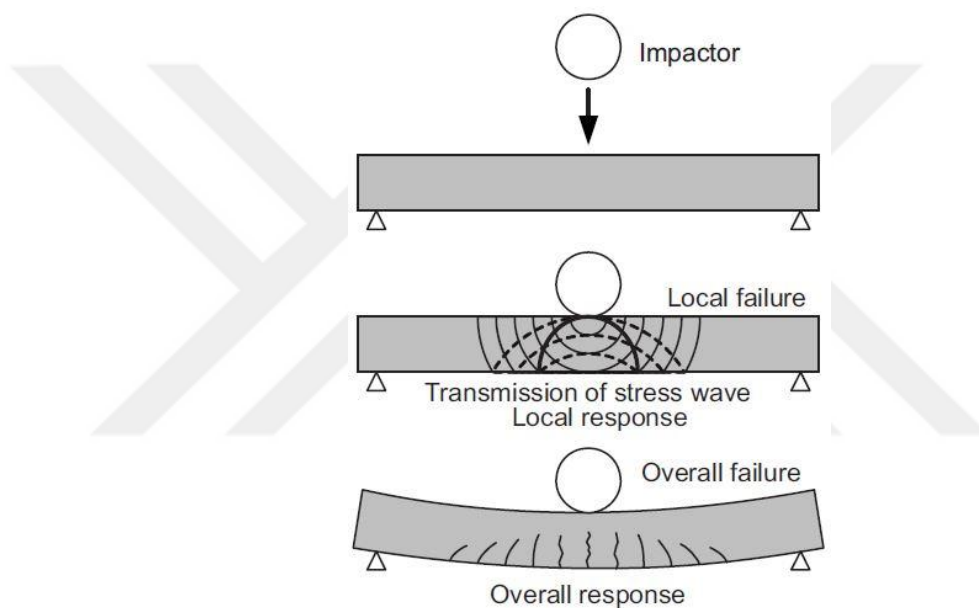


**Figure 3.10** Impact responses of a RC member [22]

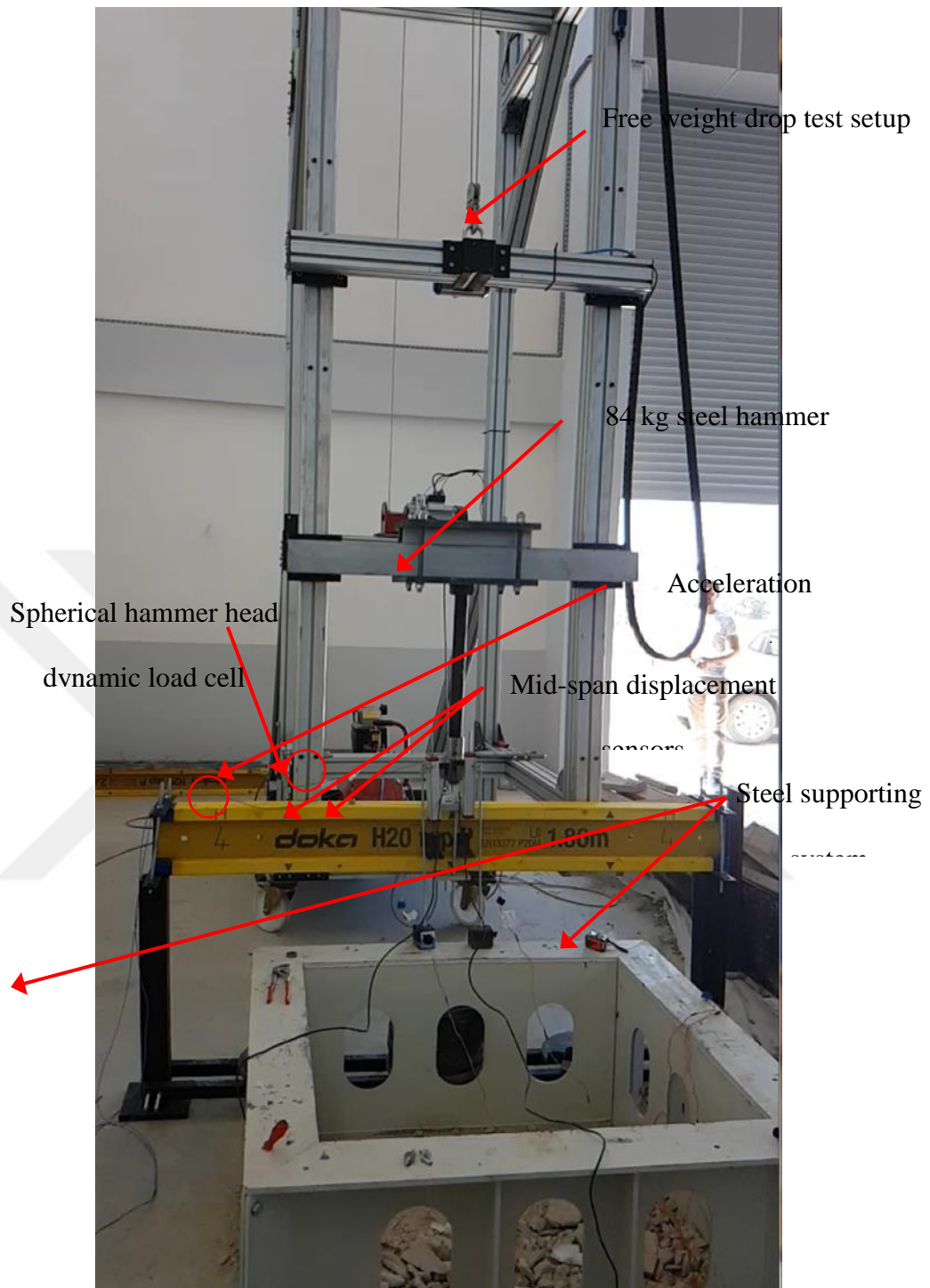


**Figure 3.11** Free weight drop test setup for impact load

In order to accurately measure the impact forces generated by the pressure force used in the impact test, a load cell with model number 200C50 produced by PCB Group was used on the test setup. Reproducibility and linearity are quite good. The load cell used in the experiment is presented in Figure 3.12. Load cell connection needs to be made correctly. The load cell is combined with the Beryllium-Copper screw which is

a high hardness material to make this connection durable and healthy. Location and image of the load cell with model number 200C50 produced by PCB Group presented in Figure 3.13.



**Figure 3.12** Load cell with model number 200C50 produced by PCB Group

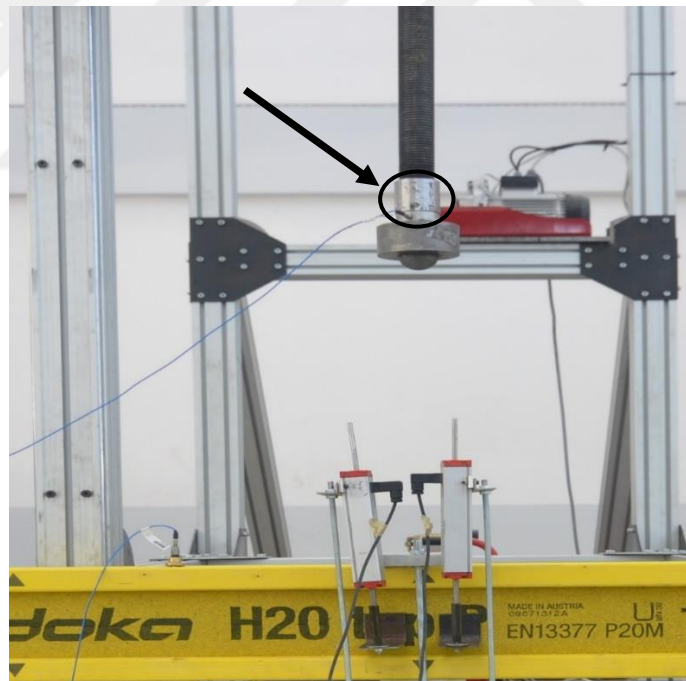


**Figure 3.13** Mounting of the load cell on the impact test

In this study, one ICP 352B70 model piezoelectric accelerometers produced by PCB Group were used. The piezoelectric accelerometer produced by the PCB company with the model number ICP 352B70 on impact test is given in Figure 3.14. Piezoelectric accelerometers must be mounted correctly on the test specimen in order to obtain

accurate measurements. The mounting of piezometric accelerometers which is a sensitive subject, was made as “Stud Mount” shown in Figure 3.15 and the accelerometers were assembled with screw and brass apparatus to detect high frequencies with high precision.



**Figure 3.14** Piezoelectric Accelerometer PCB Group ICP 352B70 Model

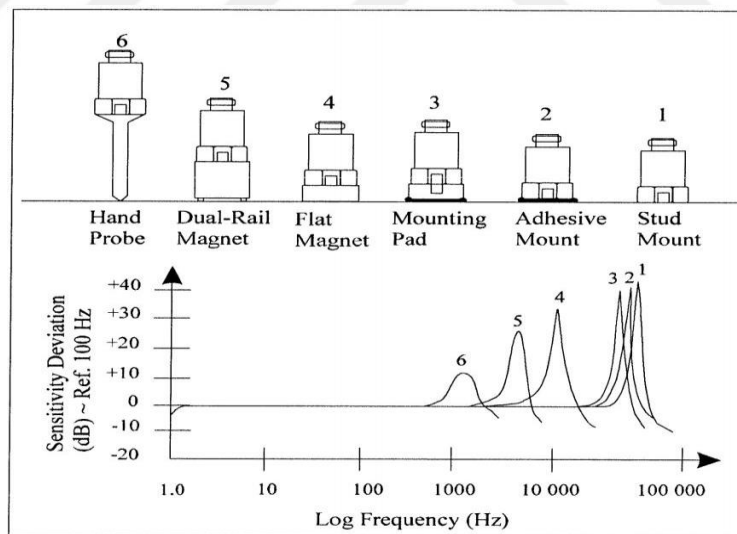


**Figure 3.15** Correct mount methods of piezoelectric accelerometers [23]

In order to obtain the highest sensitivity at the highest frequencies, the specified mounting style was applied to the specimens and the mounting form is shown in Figure 3.16.

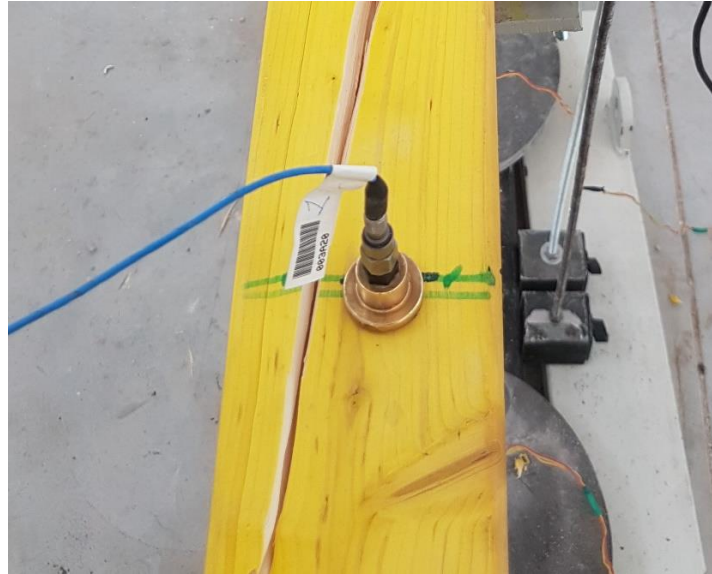


**Figure 3.16** Mounting of piezoelectric accelerometer on test specimens

LPS100 Model Linear Potentiometer (LVDT) produced by Opkon company was used to measure the displacements of the test specimens subjected to impact loading and shown in Figure 3.17.



**Figure 3.17** The LPS100 Model Linear Potentiometer of Opkon Company (LVDT)

The LVDT which are very sensitive about the displacement measurement is screwed into the body of the timber beams to be tested. Two LVDT are mounted to the central part of the beam on the left and right sides of the body where the hammer is applied in order to measure the largest displacement and fixed on the steel apparatus which is independent of the impact. The details of LVDT which is mounted on the test setup are presented in Figure 3.18.

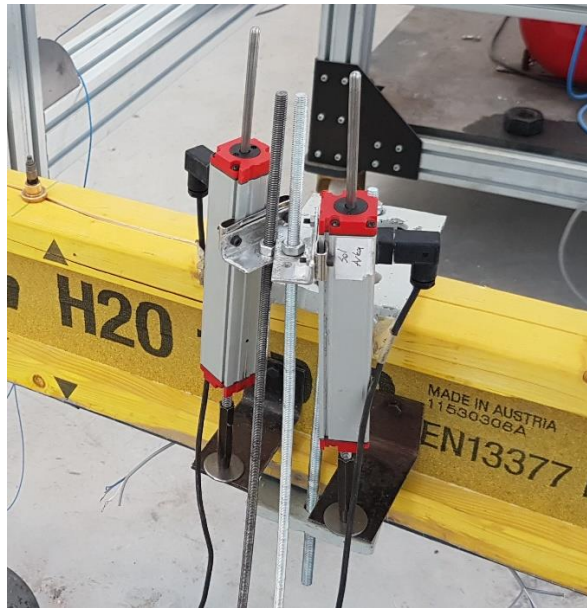


**Figure 3.18** Installation of Linear Potentiometer (LVDT)

Data logger devices NI 9234, NI 9235 and NI 9201 which were produced by National Instruments company were used in this study to make the values taken from the load cell, piezoelectric accelerometer, strain gauges and LVDT to be discarded to the computer via connecting cables. The NI 9234 data logger was used to transfer data from load cell and accelerometers to computer while the NI 9235 data logger was used to transfer data from strain gauge to the computer. Also, the NI 9201 data logger was used to collect the displacement values measured from the LVDT. Data loggers figures given in figure 3.19-a, 3.19-b and 3.19-c, respectively. The technical specifications for the NI 9234 model numbered data logger are presented in Table 3.8 as well.

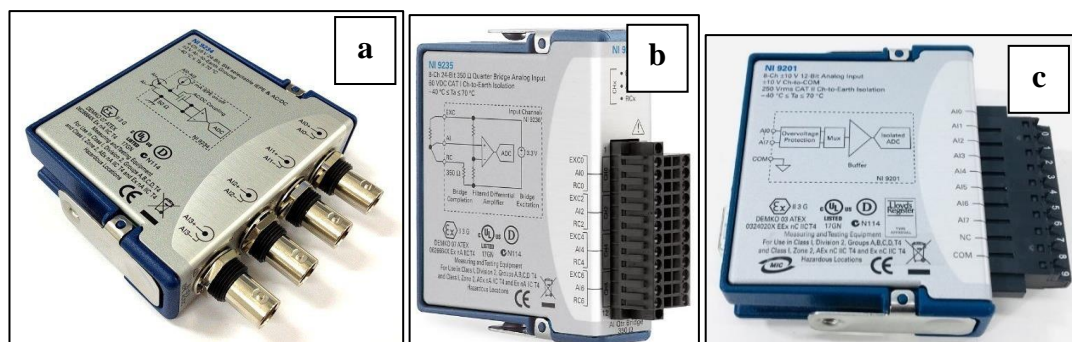


**Figure 3.19** (a) NI 9234 (b) NI 9235 (c) NI 9201

**Table 3.9** Technical Specifications for the Data Logger NI 9234

Technical Specifications	Values and Units
Number of channels	8 Channel
Resolution	24-Bit
Maximum data rate	10 kS/s/ch
Circuit completion resistance	120 $\Omega$
Working temperature	Between -40°C and + 70°C

Specimen 3, Specimen 4 and Specimen 5 with 1.80 m length were less damage after the impact test and and post-experiment photographs are shown in Figure 3.20, Figure 3.21 and Figure 3.22, respectively. Beside, damage and fractures on the timber beams for Specimen 8, Specimen 9 and Specimen 10 with 2.45 m length after the impact test are shown in Fig. 3.23, Fig. 3.24 and Fig. 3.25, respectively.



**Figure 3.20** Failure Mode of Specimen 3



**Figure 3.21** Failure Mode of Specimen 4



**Figure 3.22** Failure Mode of Specimen 5



**Figure 3.23** Failure Mode of Specimen 8



**Figure 3.24** Failure Mode of Specimen 9



**Figure 3.25** Failure Mode of Specimen 10

### 3.4.3 Damage Process and Retrofitting with CFRP Strips and Anchor

In this thesis study, there are test specimens that are damaged and then retrofitted with CFRP anchor and CFRP strip. Damage and retrofitting operations mentioned in this section. The damage process graphs of the 1.80 and 2.45 m length beams are shown in Figure 3.26 and 3.27, respectively.

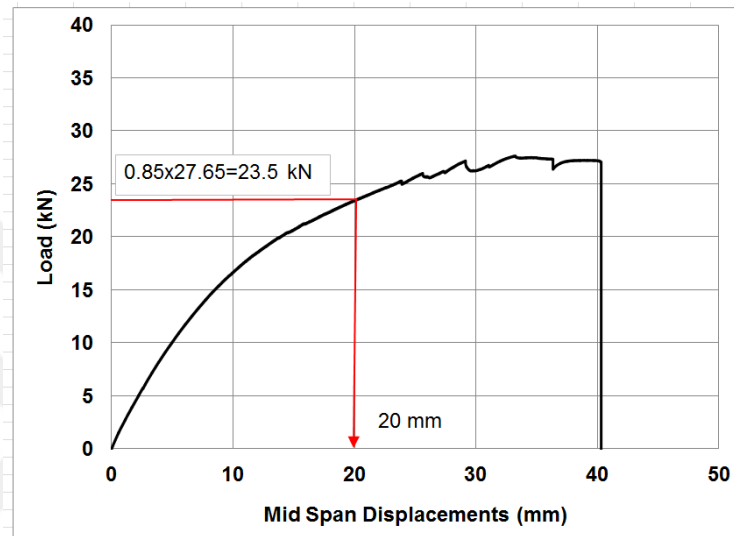


Figure 3.26 Damage Limit of 1.80 m Timber Beam

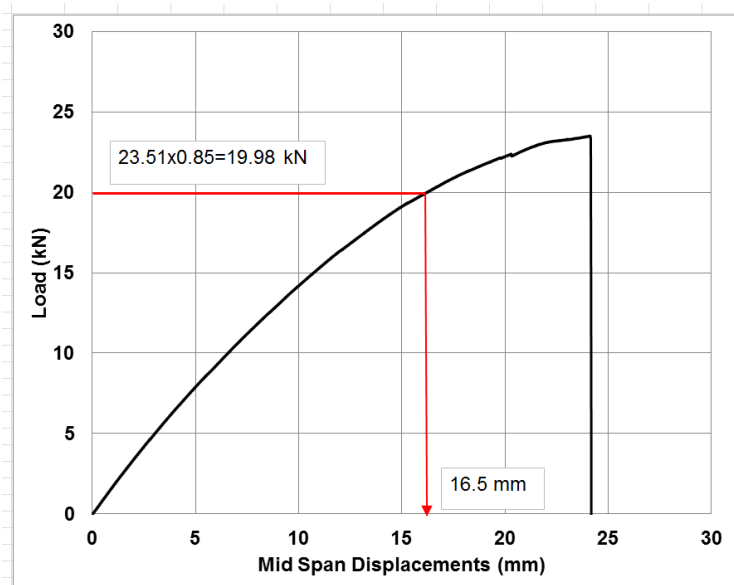


Figure 3.27 Damage Limit of 2.45 m Timber Beam

Timber beams were exposed to load up to 23.5 kN for 180 cm beam, up to 19.98 kN for 245 cm beam and then the experiment was stopped.

After the damage process, CFRP was cut according to the strip size as shown in figure 3.28. CFRP anchors are also prepared as shown in figures 3.29.



**Figure 3.28** Cutting of CFRP Strips

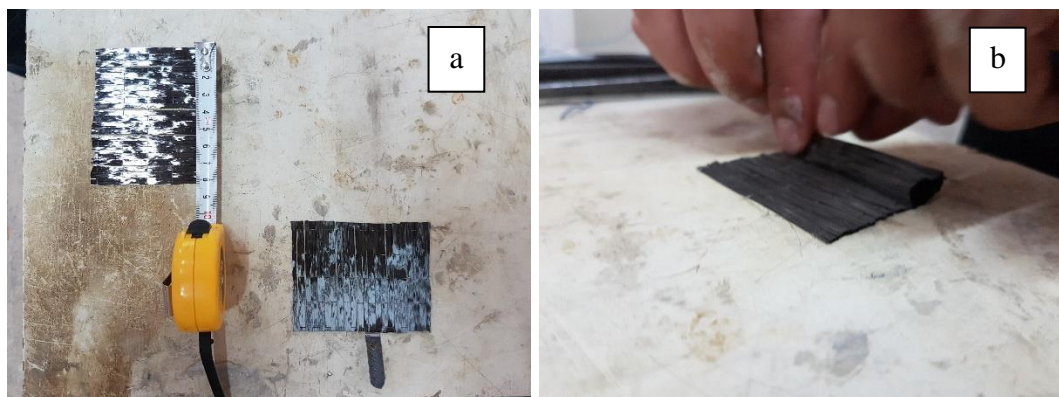


**Figure 3.29** (a) CFRP Anchor Diameters (b) CFRP Wrap on Iron Piece ( $\phi 8$ )

After the CFRP strips and anchors were prepared, holes were opened on the timber beams as shown in figures 3.30.

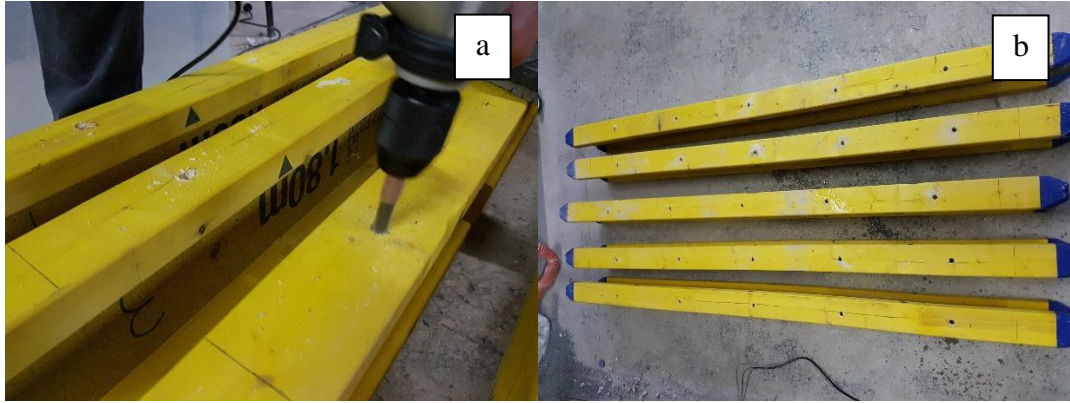


**Figure 3.30** (a) Making a Hole in Timber (b) Drilled Timber Beams

After the drilled beams were cleaned with a wet cloth, the epoxy was prepared as in figure 3.31(a) and the CFRP strips were glued as in figure 3.31(b).

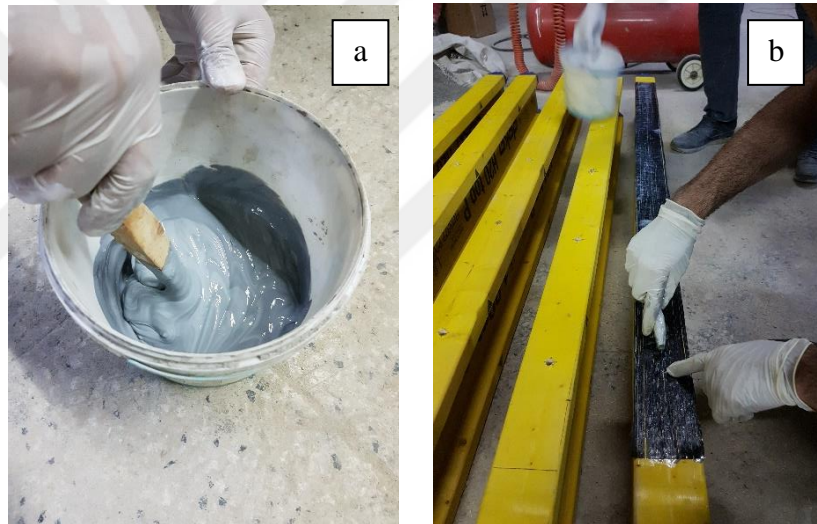


**Figure 3.31** (a) Preparation of Epoxy (b) CFRP Bonding

After the CFRP is bonded, the anchorage holes are opened as shown in Figure 3.33 and the anchors are nailed on timber by injecting epoxy into the anchorage holes. After the CFRP Anchors nailed as show in figure 3.34, it is bonded as fan type on CFRP. Fan type anchor details given in the figure 3.32.

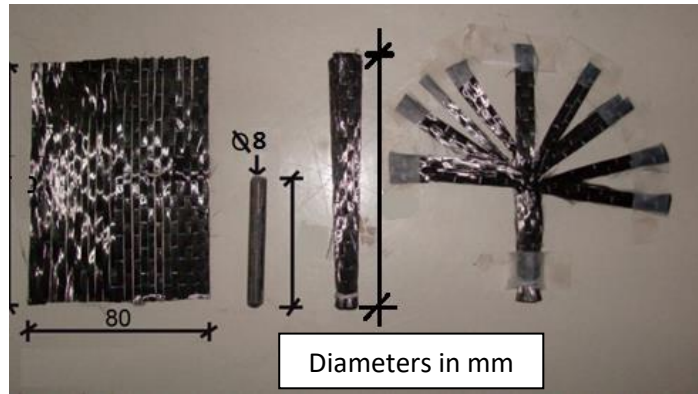


**Figure 3.32** Details of CFRP Fan Type Anchor



**Figure 3.33** (a) Finding the Drill Hole (b) CFRP Anchors

Fan type anchor application is given in figure 3.34(a) and the timber beams which retrofitted with CFRP image is shown in figure 3.34(b).



**Figure 3.34** (a) Fan Type CFRP Application (b) Retrofitting with CFRP

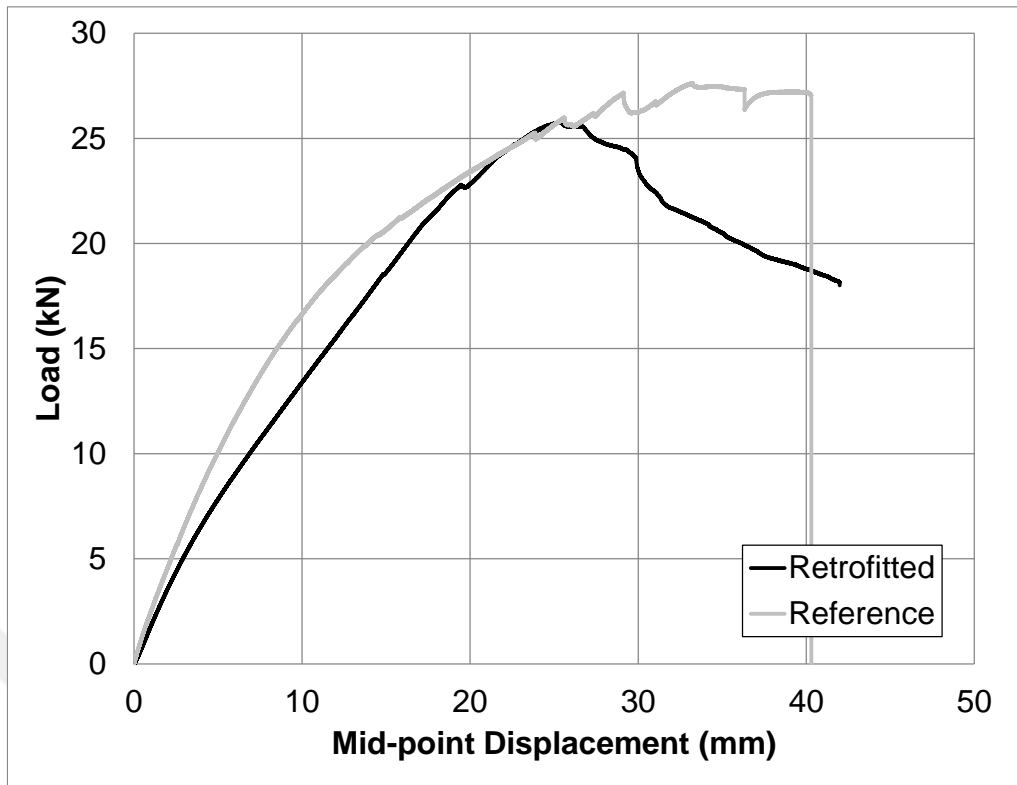
**CHAPTER 4**  
**EXPERIMENTAL RESULTS AND DISCUSSIONS**

**4.1 Static Loading Results**

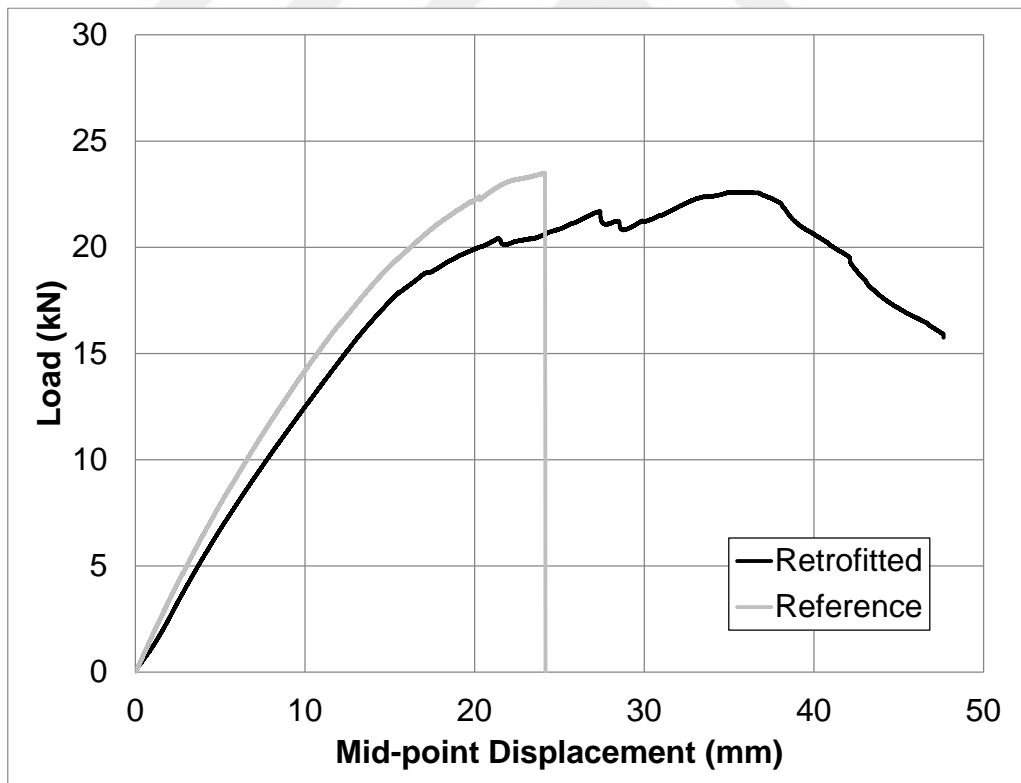
In the experimental study, first of all the tests of damaged retrofitted timber formwork beams under monotonic increased static loading effect were performed and the load-displacement behaviors of the beams were obtained. The load-displacement graphs obtained as a result of the tests of the Specimen 1 with 1800 mm length and Specimen 6 with a length of 2450 mm are given in Figure 4.1 and the results are given in Table 4.1. In addition, for the maximum load level, the distribution of the strain values measured on the CFRP fan type anchored CFRP strips bonded to the tension surface of the damaged beams for repair purposes is given in Figure 4.2. By using the load-displacement graphs obtained as a result of the experiments, the maximum carrying capacity values, initial stiffness, displacement ductility ratios and energy dissipation capacities of the experimental elements were calculated and determined. Displacement ductility ratio values were defined as the point where the maximum carrying capacity of the test specimens decreased by 15% to at a level of 85% and the displacement value of this point is calculated by proportioning the maximum carrying capacity to the displacement value. The energy dissipation capacity values of the test specimens was obtained by calculating the area of the load-displacement graphs below the parts up to the collapse point. The point of displacement is identical to the point of collapse and used for displacement ductility rates. The methods used to determine the calculated values for the test specimens are presented in Figure 4.3.

**Table 4.1** Experimental Result for Static Loading Test

<b>Spec. No</b>	<b>Ultimate Load (kN)</b>	<b>Displacement at Ultimate Load (mm)</b>	<b>Initial Stiffness (kN/mm)</b>	<b>Ductility Ratio</b>	<b>Energy Dissipation Capacity (kN-mm)</b>	<b>Maximum Strain (mv)</b>
1	25.81	25.27	1.59	1.28	754.03	0.0122
6	22.61	35.43	1.29	1.19	808.87	0.0172

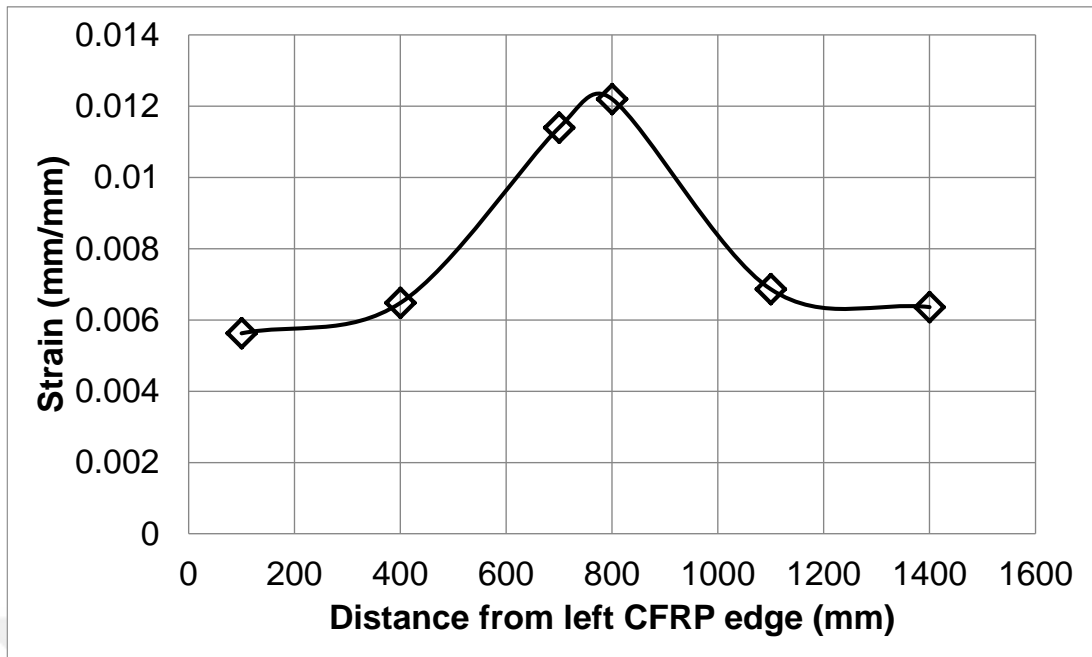


a) Specimen-1 monotonous static load-displacement graph

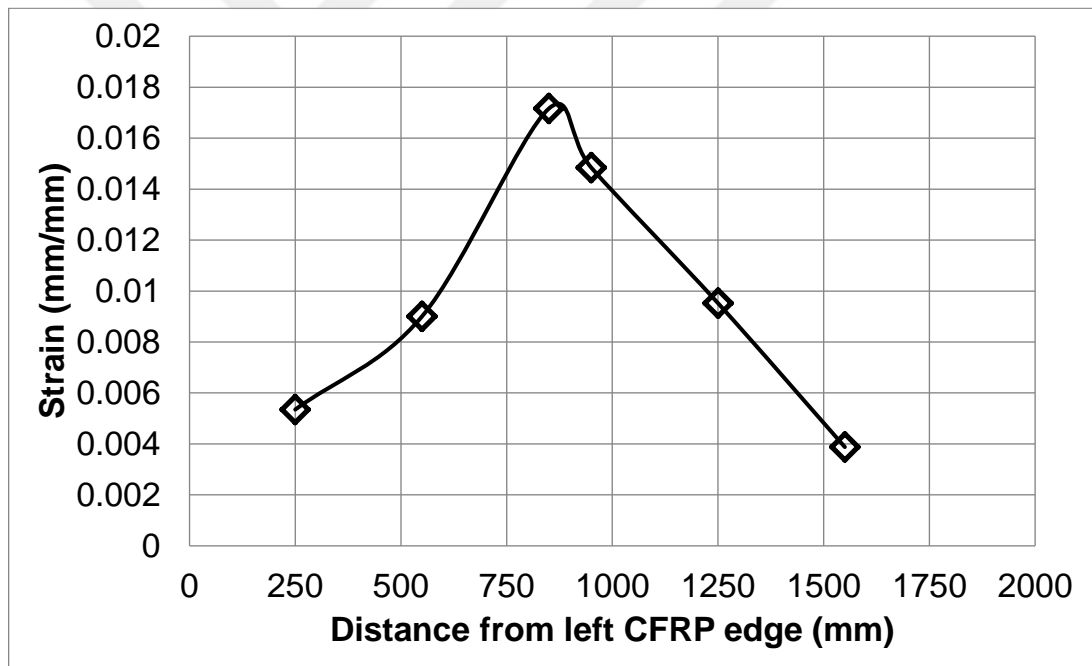


b) Specimen-6 monotonous static load-displacement graph

**Figure 4.1** Static Load-Displacement Graphs of Specimens



a) Specimen-1 strain distribution along to CFRP strip



b) Specimen-6 strain distribution along to CFRP strip

**Figure 4.2** Strain Distribution Graphs of Specimen for Static Load at Ultimate Load Level

When the test results were examined, it was observed that the Specimen 1 with 1800 mm span had a maximum carrying capacity of 14% more than the Specimen 6 with 2450 mm span and reached 40% more displacement to this load level. Specimen 1 achieves maximum carrying capacity with less displacement and more ductile

behavior, as well as 23% more initial stiffness than the Specimen 6. The displacement ductility rate of the Specimen 1 is 8% greater than the Specimen 6. Since the Specimen 6 reached a maximum displacement value with a much higher displacement, the energy dissipation capacity was calculated as a small percentage of 7% from the Specimen 1. In general, it was observed that the behavior of the damaged retrofitted Specimen 1 was better than the Specimen 6 under static loading, and showed a load-displacement behavior with high strength and rigidity as well as a more ductile behavior than the Specimen 6. Specimen 1 showed even a little higher energy consumption capacity than the experimental element due to the fact that Specimen 6 reaches maximum carrying capacity by far more displacement as well. The load-displacement graphs which described as a reference in Figure 4.1 belong to undamaged timber beam. When the load-displacement behaviors of damaged retrofitted Specimen 1 and Specimen 6 compared with undamaged reference test specimens it was observed that the repair technique applied to the test specimens of two different lengths gives very successful results. Both of the test specimens were obtained with a rigidity similar to the approximate maximum carrying capacity with the undamaged reference test specimens, and the damaged retrofitted Specimen 6 exhibited a much more ductile behavior and exhibited greater energy dissipation capacity than the undamaged reference test specimen. When the strain distributions taken on the CFRP strips bonded to the tensile surfaces given in Figure 4.2 for retrofitted Specimen 1 and Specimen 6 are examined, it is seen that the strain values in both test elements reach the maximum value in the axis of symmetry where the loading is applied at the mid point of the beam. The maximum strain value measured at the mid-point of the Specimen 6 was 41% higher than the Specimen 1. This result showed that more load is carried by the anchored CFRP strip used for repair in the Specimen 6. The use of anchors prevented the slipping of the CFRP strips from the surface and increased the maximum strain values measured from the CFRP strips by increasing the 0.005 mm / mm limit value given as the slipping limit value for the CFRP material in the ACI 440 R1-17, 2017 committee report. Maximum strain values measured under the effect of static loading from the damaged test specimens retrofitted with anchored CFRP strips were obtained on average 194% larger than the slipping strain value for CFRP strips given in ACI 440 R1-17 committee report.

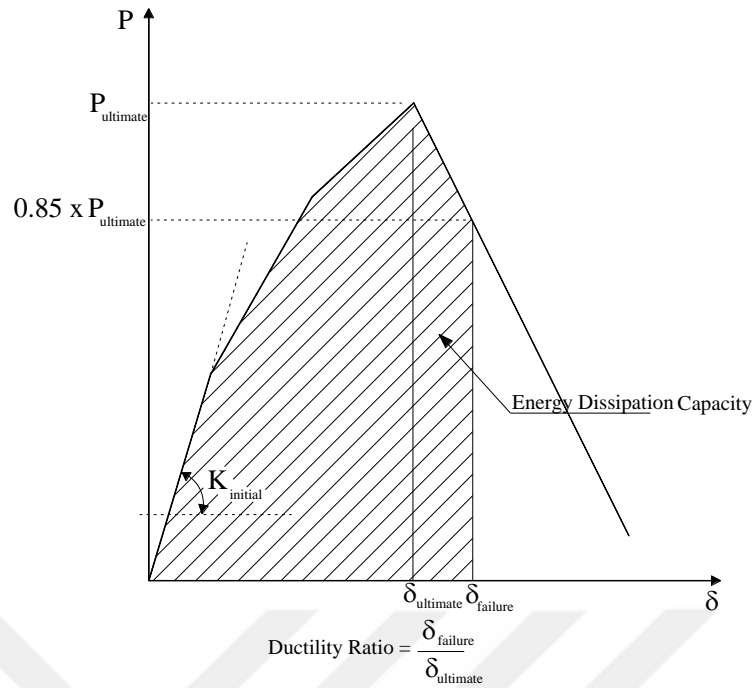


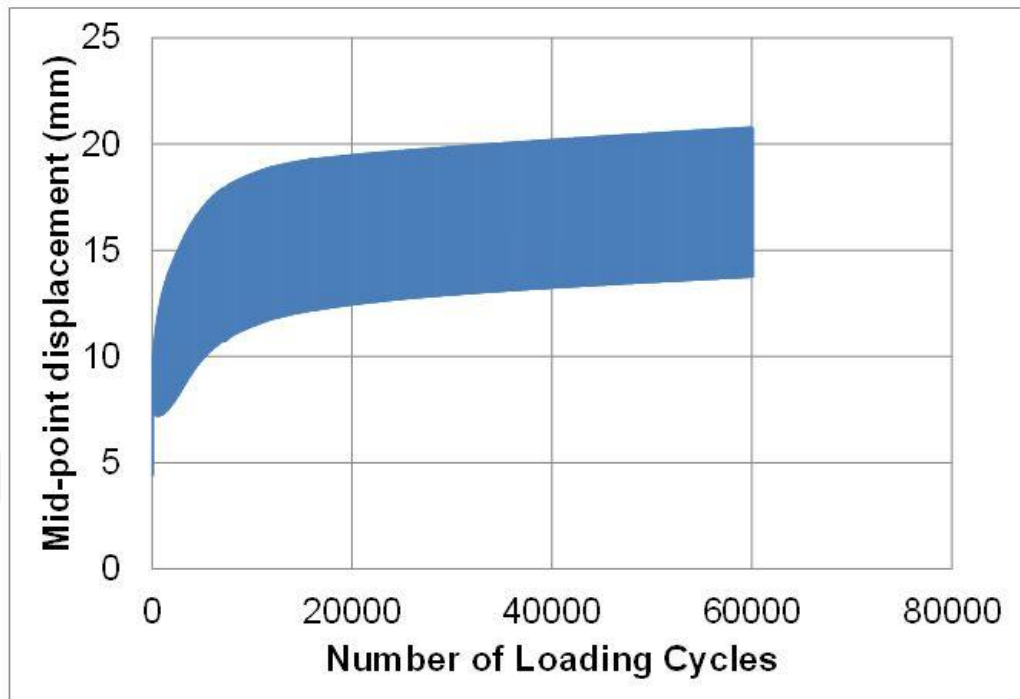
**Figure 4.3** Calculation Approach of Ultimate Load Capacity, Initial Stiffness, Displacement Ductility Ratios and Energy Dissipation Capacity

## 4.2 Fatigue Loading Results

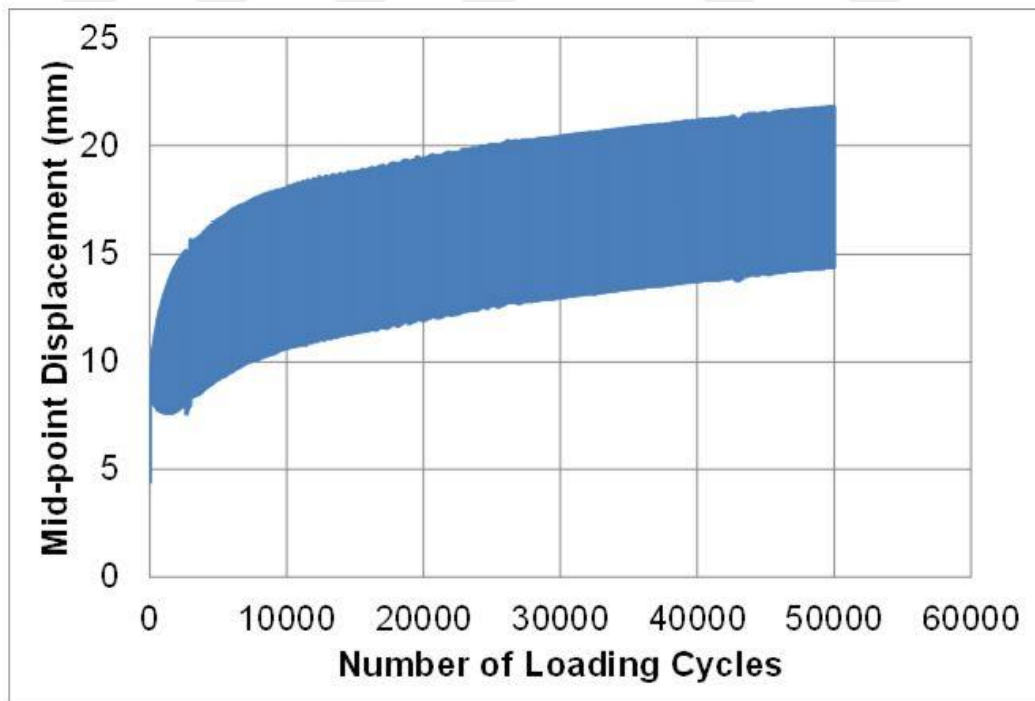
The second type of installation examined in the study is a high load low cycle fatigue loading. The profile of fatigue loading applied to the Specimen 2 damaged repaired timber beam of 1800 mm length was determined using the results obtained from the Specimen 1. The maximum and minimum load levels in the fatigue loading profile applied to the Specimen 2 were determined as 10% and 85% of the maximum carrying capacity of Specimen 1, respectively. As a result of the 60000 loading cycle applied to the specimen 2, the specimen has failed and the test has been completed. While the mid-point displacement of the beam is 4.45 mm when the fatigue load is applied to the Specimen 2, mid-point displacement increased up to 20.71 mm just before failing. While damaged retrofitted Specimen 1 with the same properties displace 17.6 mm at 21.94 kN load level under the effect of static loading, displacement at the same load level under the effect of fatigue loading was 18% more as a result of the 60000 loading cycle. The amount of change in beam mid-point displacement increased up to 5.81 mm at the end of the test when loading value varies between maximum and minimum values under the effect of fatigue loading profile applied to Specimen 2. The damaged

retrofitted Specimen 7 tested by fatigue loading is identical to the Specimen 6 tested under static loading. The maximum and minimum values of the fatigue loading applied to the Specimen 7 were determined similar to the beam test specimen with a length of 1800 mm as 85% and 10%, respectively, of the maximum carrying capacity of the Specimen 6. The fatigue loading applied to the Specimen 7 failed after the 50000 loading cycles and the test has been terminated. At the beginning of the experiment, when the mid-point displacement value of the Specimen 7 was 4.42 mm, after the 50000 loading cycle the mid-point displacement of the beam increased to 21.81 mm just before failing at the test result. The mid-point displacement of the beam increased to 20% more just before the failing on the Specimen 7 tested under the influence of fatigue loading at the end of the test, the beam mid-point displacement value of the same 19.22 kN load level is 18.19 mm in the Specimen 6 tested with static loading effect on identical properties. The difference between the maximum and minimum load levels of the beam mid-point displacement values increased up to 7.31 mm before failing under the influence of fatigue loading applied to the Specimen 7 at the end of the test. The displacement graphs obtained as a result of the fatigue tests applied to the Specimen 2 and Specimen 7 are given in Figure 4.4 and the test results are given in Table 4.2. Undamaged 1800 and 2450 mm long timber beam test specimens under high load level fatigue loading has achieved much more displacement in the number of low cycles than retrofitted with damaged anchored CFRP strips test specimens. Undamaged timber beams of 1800 mm and 2450 mm length have failed through the loading cycle of 3372 and 4339 respectively, and the beam mid-point displacement values have reached 46.58 mm and 31.92 mm, respectively. Damaged, retrofitted with anchored CFRP strips 1800 and 2450 mm long timber beam test specimens, on the other hand, resist on a much longer time fatigue loading as a result of 17.8 times and 11.5 times more loading cycles, respectively. Undamaged 1800 mm and 2450 mm long beams have more displacement of 125% and 46% than the damaged retrofitted beams, respectively. The retrofit technique applied with anchored CFRP strips has reduced the mid-point displacement of the beam due to fatigue loading much more successfully and has significantly reduced. In addition, the distribution of the strain values measured on CFRP fan-type anchored CFRP strips bonded to the tension surface of damaged beams for repair purposes is given in Figure 4.5 at the end of the test. When the strain distributions measured along CFRP strips bonded to the beam tension surface for

repair are examined, it is seen that the maximum strain values occur at the mid point of the beam where fatigue load is applied.



a) Specimen-2 displacement-number of loading cycles graph for fatigue load



b) Specimen-7 displacement-number of loading cycles graph for fatigue load

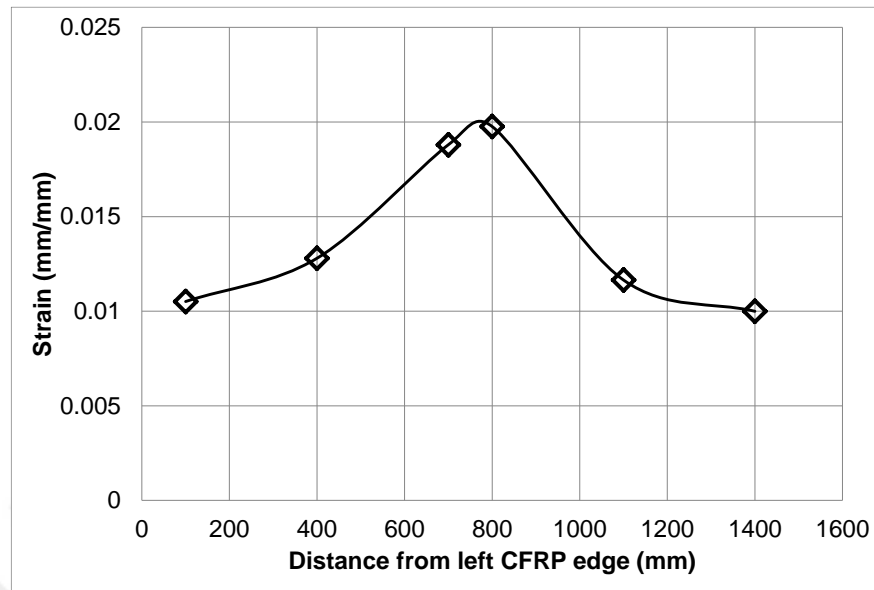
**Figure 4.4** Displacement Changing Graphs of Specimens under Fatigue Load

**Table 4.2** Experimental Result for Fatigue Loading Test

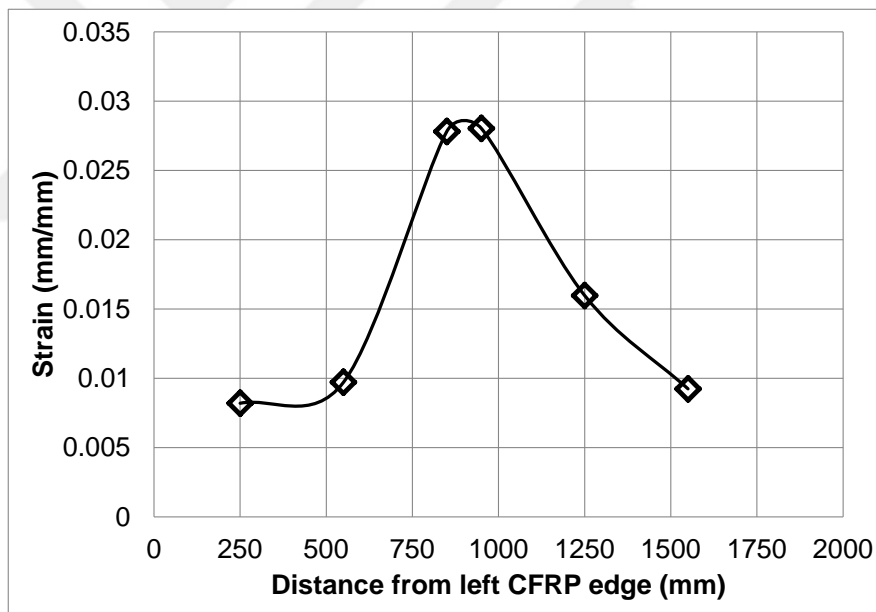
Spec. No	Fatigue Load (kN)		Displacements (mm)		Number of Loading Cycles	Maximum Strain (mv)
	Maximum	Minimum	At Failure	At Beginning		
2	21.94	2.58	20.71	4.45	60000	0.0198
7	19.22	2.26	21.81	4.42	50000	0.0280

Maximum strain values measured from damaged retrofitted timber beams tested under the effect of fatigue loading are obtained as 378% greater than 0.005 mm / mm surface slipping strain limit value given for CFRP strips in ACI 440 R1-17 committee report. The result showed that CFRP strips which are used for retrofitting are able to take significant axial tensile stresses with the effect of fatigue loading and they were able to reach much larger strain values without being slipped off the surface by the effect of anchors. The retrofit technique applied with anchored CFRP strips effectively limited the deformations of the damaged timber beams under fatigue loading and the CFRP strips carry an axial tension force without slipping off the surface, allowing more carrying load cycle than undamaged reference beams. When the behavior of the Specimen 2 with 1800 mm length and Specimen 7 with 2450 mm length tested under the effect of fatigue loading, it has been seen that the Specimen 2 has a more successful performance. Specimen 2 has 5% less displacement than the Specimen 7 and 20% more fatigue loading has carried the load up to the number of cycles without failing at the end of the test. Moreover, the Specimen 2 withstand more loading cycles by making less displacement while the maximum strain value measured from the CFRP strip remained at a lower level than the Specimen 7. The maximum strain value measured from the CFRP strip of Specimen 7 is 41% greater than the Specimen 2. These results showed that the applied retrofit technique performed in the Specimen 2 which was tested under the effect of fatigue loading with 1800 mm length showed a more successful performance than the Specimen 7 with a length of 2450 mm. Also, the maximum strain values measured from CFRP strips in Specimen 2 and Specimen 7 were measured an average of 63% more compared with Specimen 1 and Specimen 6 tested under static loading. Obtained this result showed that CFRP strips had more

axial tensile stress than static loading and they were used more effectively to achieve more performance on the repair techniques applied in the fatigue loading.



a) Specimen-2 strain distribution along to CFRP strip



b) Specimen-7 strain distribution along to CFRP strip

**Figure 4.5** Strain Distribution Graphs of Specimen for Fatigue Load at the end of Test

### 4.3 Impact Loading Results

In the experimental study, impact loading was applied to the damaged retrofitted timber formwork beam test specimens having 1800 and 2450 mm spans as the third loading type. The tests were carried out 84 kg weight of hammer dropping from 3 different heights in order to apply the impact load applied to the test specimens at 3

different energy levels. In the experimental program, firstly, Specimen 3, 4, and 5 with 1800 mm span were subjected to impact loading with 500, 750 and 1000 mm height, respectively. Similarly, impact tests were carried out also on Specimen 8, 9, and 10 by dropping the constant weight hammer from 500, 750 and 1000 mm height, respectively. The left acceleration-time, left and right displacement-time, maximum strain-time and applied impact loading-time graphs are shown in Figure 4.6, 4.7, 4.8 and 4.9, respectively, and test results obtained from the impact tests applied to the test specimens are given in Table 4.3. In addition, the strain distributions measured along CFRP strips bonded to the tension surface of the beams for retrofit purposes are shown in Figure 4.10 for the maximum load value by the effect of impact loading.

When the test results of Specimen 3, 4 and 5 with 1800 mm span are examined, as a result of the increase in the impact energy and load applied to the test specimens with the increased drop height, the maximum acceleration values measured from the test specimens, the mid-point displacement values of the beam, and the maximum change of the strain values of the beam-tension surface all increased. Specimen 5 tested by applying a drop from a height of 1000 mm exhibited more maximum acceleration, maximum left displacement, maximum right displacement and maximum strain values of 35%, 38%, 39%, and 31%, respectively than the Specimen 4 tested with a height of 750 mm. The impact load applied to the Specimen 5 is 40% greater than the Specimen 4. Specimen 4 tested with a 750 mm drop height had more maximum acceleration, maximum left and right displacement and maximum strain values of 41%, 36%, 44%, and 36%, respectively than the Specimen 3 tested with a height of 500 mm. Similar behavior trend was observed in Specimen 8, 9 and 10 test specimens with 2450 mm span as well. The maximum acceleration, maximum displacement, maximum strain values measured from the test specimens all increased significantly as a result of the increase of the impact height and the increase of the impact energy applied. Specimen 10 tested with a 1000 mm drop height displayed more maximum acceleration, maximum left displacement, maximum right displacement and maximum strain values of 34%, 37%, 37%, and 31%, respectively than the Specimen 9 tested with a height of 750 mm. The impact load applied to the Specimen 10 is 41% greater than the Specimen 9. Specimen 9 tested with a 750 mm drop height had more maximum acceleration, maximum left and right displacement and maximum strain values of 41%, 34%, 34%, and 36%, respectively than the Specimen 8 tested with a height of 500 mm.

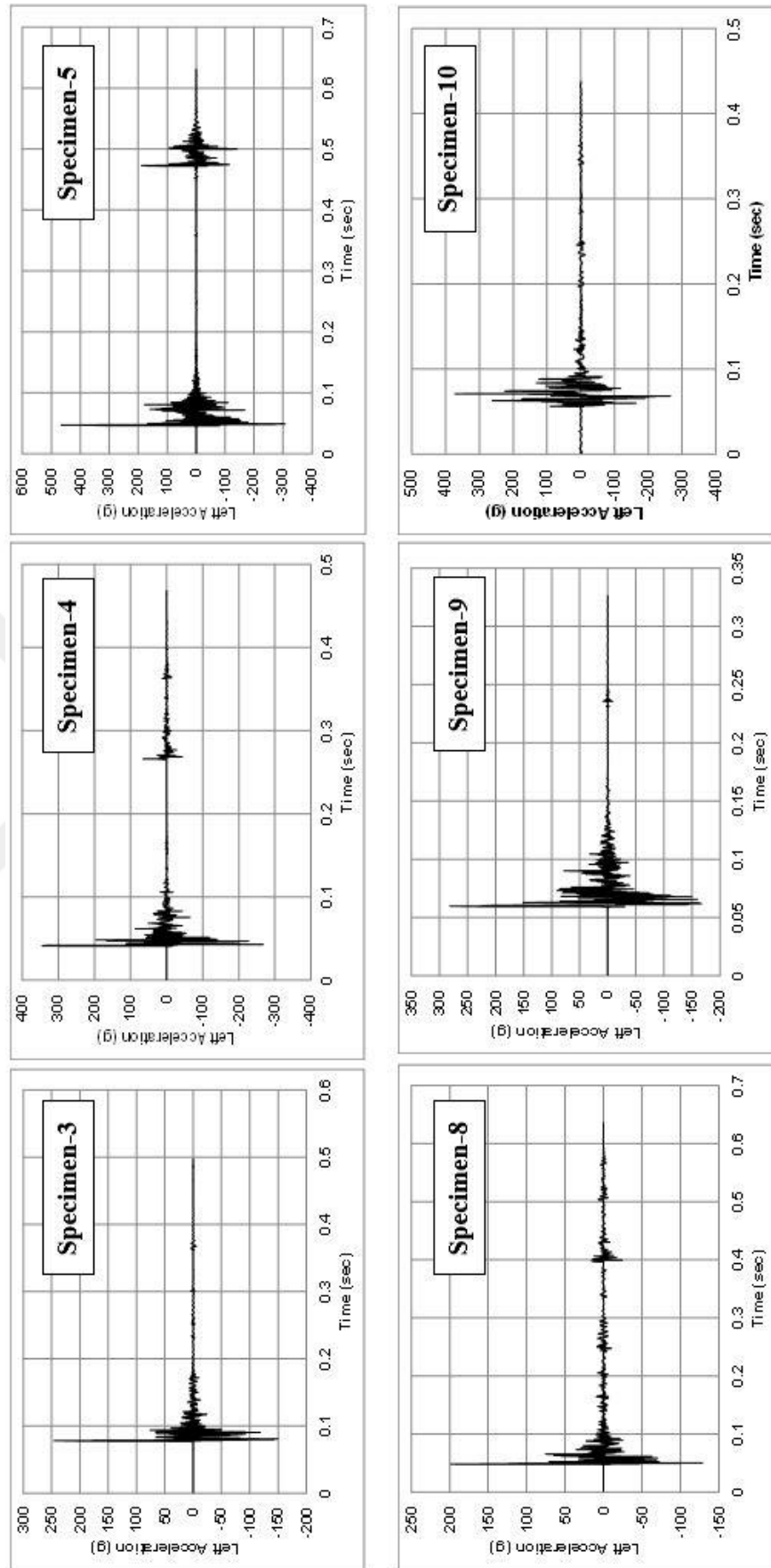


**Figure 4.6** Left Acceleration-Time Graphs of Specimens under Impact Load

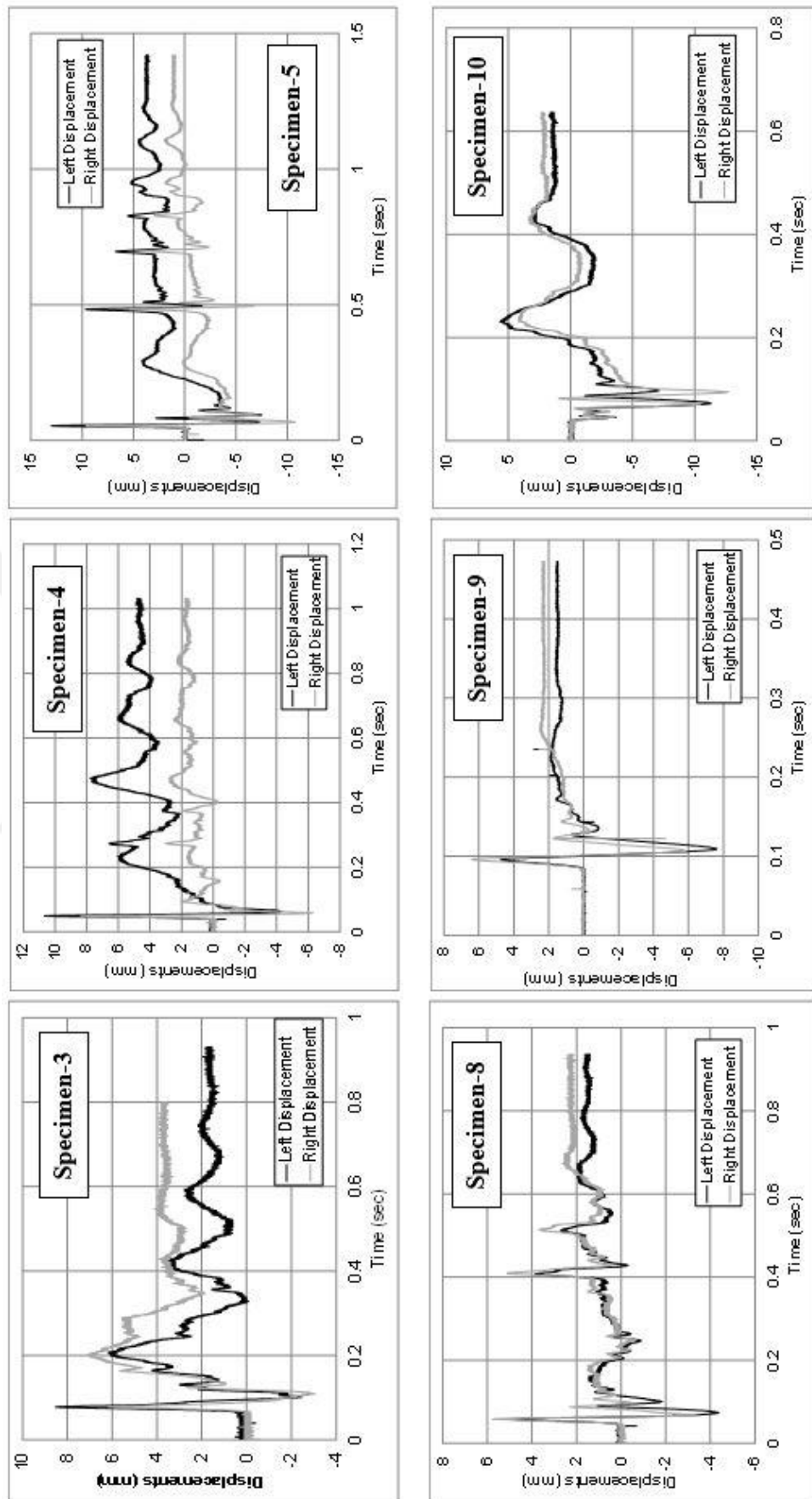


**Figure 4.7** Displacement-Time Graphs of Specimens under Impact Load

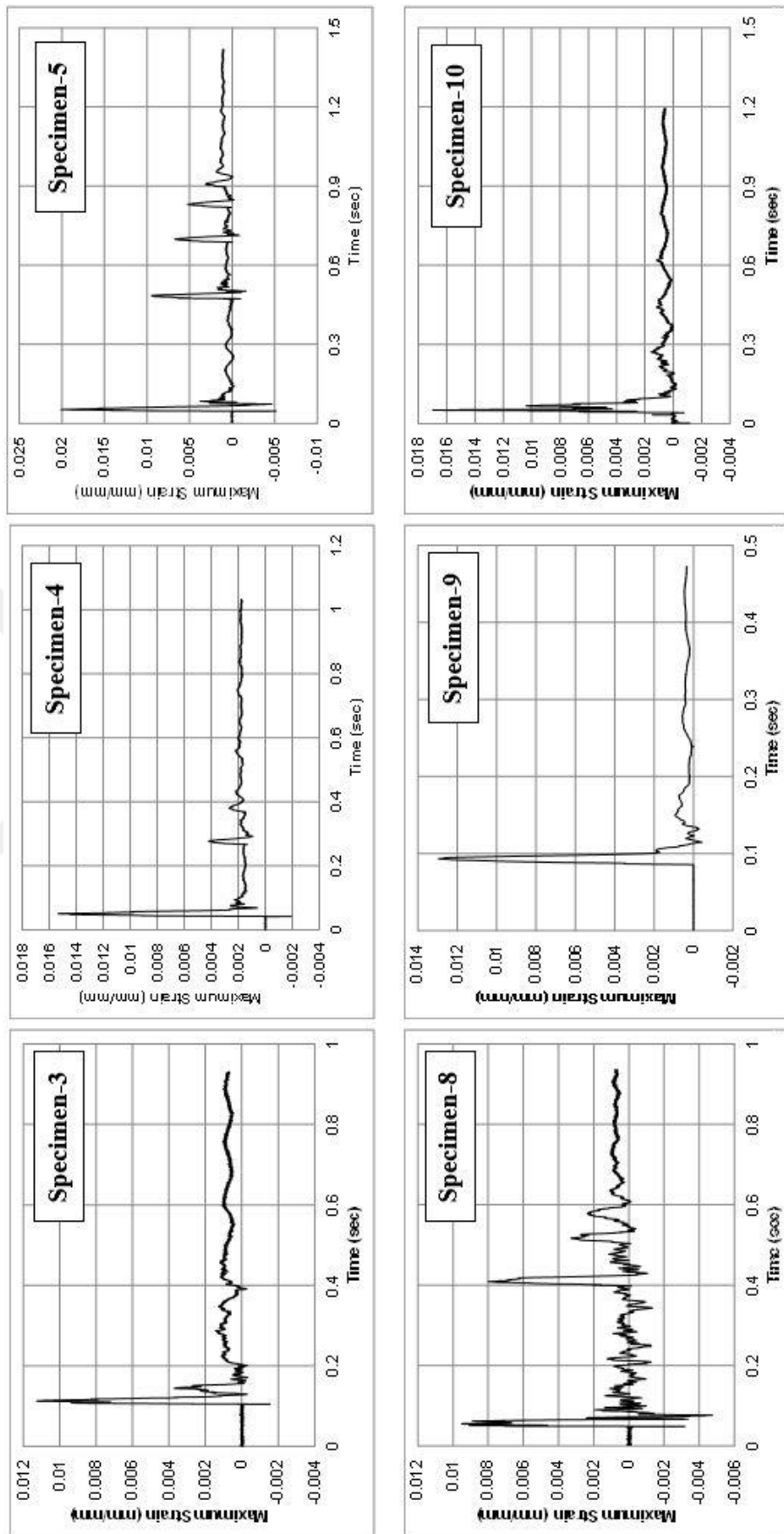


**Figure 4.8** Maximum Strain-Time Graphs of Specimens under Impact Load

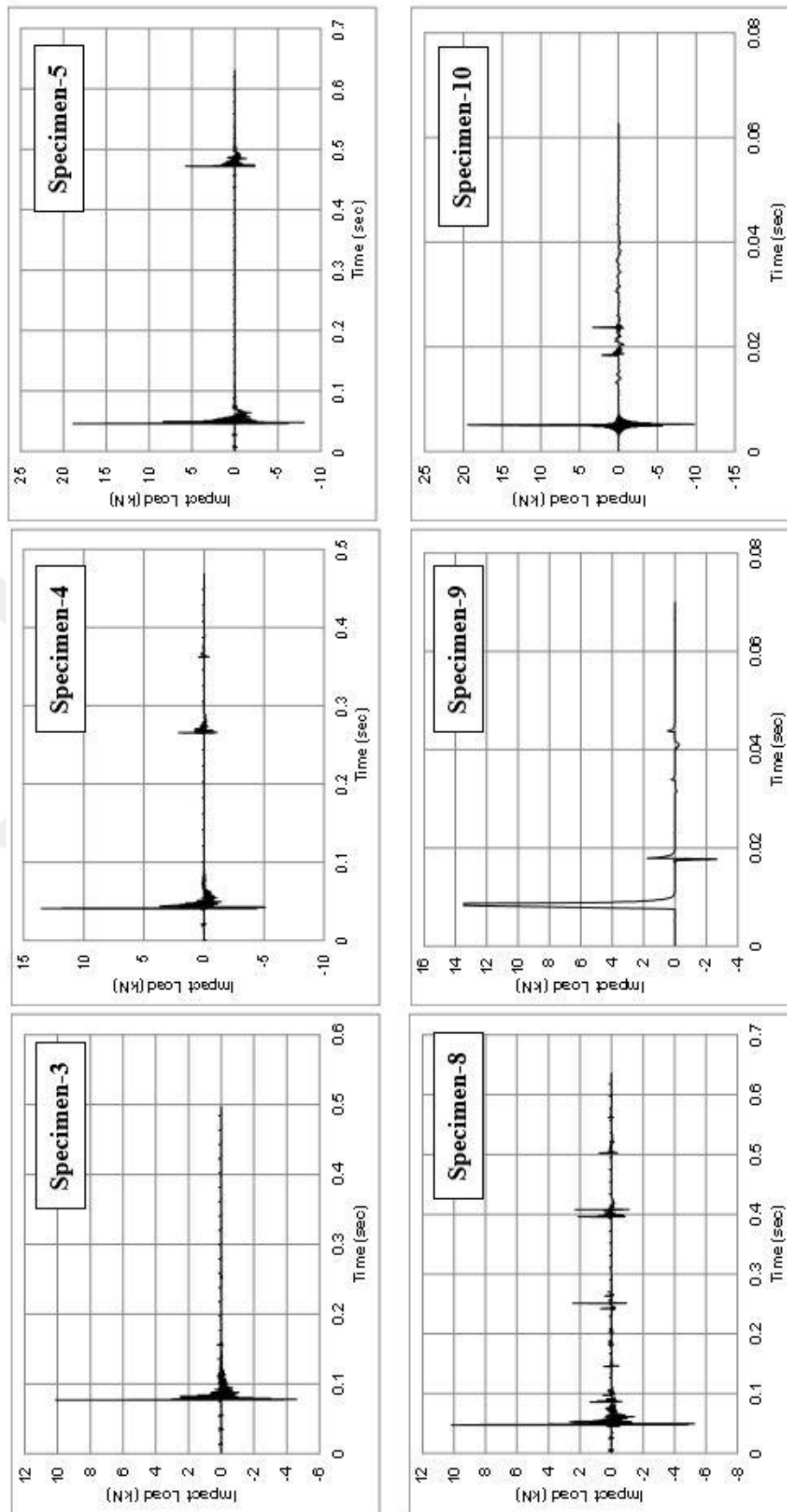


**Figure 4.9** Impact Load-Time Graphs of Specimens

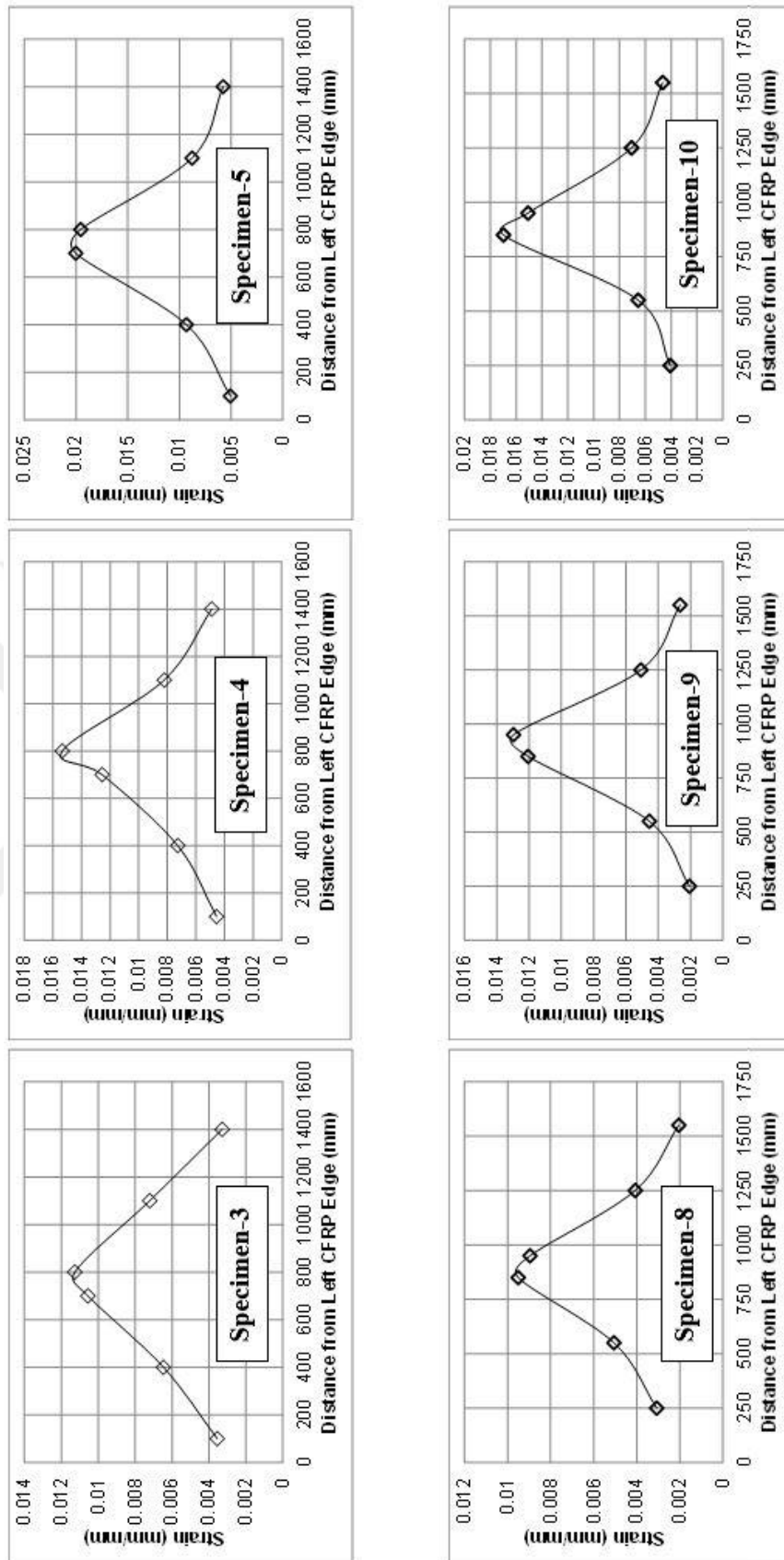


**Figure 4.10** CFRP Strain Distribution Graphs of Specimens at Ultimate Load Level under Impact Load

The maximum acceleration, maximum left and right displacements, and maximum strain values measured from the beam test specimens, all decreased when the span of damaged retrofitted timber beam test specimens increased under the effect of impact loading. The maximum acceleration, maximum left and right displacement and maximum strain values of the test specimens having 1800 mm span were obtained more an average of 24%, 20%, 17%, and 18%, respectively than the test specimens having 2450 mm span. When the graphs of strain distributions along the CFRP strip are analysed in Figure 4.10, maximum strain values have been observed at the mid-point of the beam where the impact loading is applied on damaged retrofitted timber beams. When the maximum strain values measured by the effect of impact loading were examined the resulting values were found to be greater than the average of 0.005 mm / mm from the slipping limit value given in the ACI 440 R1-17 committee report. This obtained result shows that CFRP strips carry effective axial tensile stress without slipping from the surface by the effect of impact loading in the applied retrofit technique. In this result, the CFRP fan-type anchors used on CFRP strips have played an active role and they allowed CFRP strips to carry much more axial tensile forces as they prevent slipping from the surface. When the behavior of undamaged timber beams and damaged retrofitted timber beams under impact loading is examined, they perform close to each other and the retrofit technique applied on damaged beams increases their performances of the beams under the impact loading and brings them closer to the undamaged beams. The maximum left acceleration values measured from undamaged timber beams measured as small as 10% than damaged beams and maximum left and right displacement values measured from damaged wooden beams were obtained greater 8% and 11%, respectively than the undamaged beams. Damaged beams exhibited a very close performance to the undamaged beams under the effect of impact loading.

Damage and fracture distribution after testing depending on the type of loading applied to the test specimens showed a significant change and failure mechanisms are given in Figure 4.11 by selecting the photos. When the failure mechanisms occurring in the Specimen 1 and Specimen 6 test elements tested in the static loading effect were examined, in the cross-section where the loading at the mid-point of the beam is applied, the upper pressure surface of the timber beam has crushed at the point where the load is applied at the mid-point of the beam and the crush zone has expanded with

increasing loading. As a result of the expansion of the crush zone, beams were failed by occurring cracks in the direction of parallel to the axis of the beam on the top header part of the beam. Anchored CFRP strips bonded to the tensile surfaces of Specimen 1 and Specimen 6 have not been slipped or ruptured from the surface. Anchors prevented the slipping of CFRP strips from the surface. When the failure mechanisms of Specimen 2 and Specimen 7, where fatigue loading is applied, the damage and fracture distribution in the test specimens has been shown to occur in a very similar way to the Specimen 1 and the specimen 6 tested under the static loading effect. In the first cycles where fatigue loading is applied to the test elements, a crush zone has been formed in the region where the number of loading cycles is increased and the fatigue load is applied in the top header part of the beams. Then, as the result of increased loading cycle number and mid-point displacement occurring in the beams, bending cracks were formed in the bottom tension heads of the beams close to the point where the load was fully applied and the CFRP strips bonded to the tension surface were ruptured by tearing in both test specimens at a point very close to the mid-point of the beam. When the failure mechanisms of the test specimens where the impact loading is applied were examined, the increase was seen in damage and fracture distribution occurred on the test specimens as the impact energy applied to the test specimens increased. It has been seen that crushes occur at the point where the loading is applied at the top header of beam at the mid-point of the beam, except for the fractures occurring along the beam axis and at the sections of the beams with the effect of impact loading applied. In the Specimen 5 and Specimen 10 tested by dropping from a height of 1000 mm, CFRP strips were not slipped off from any surface, but the CFRP strip was ruptured by tearing at the center of the beam where the impact loading was applied while CFRP strips do not slip or rupture from the surface in Specimen 3, 4, 8 and 9 tested with 500 mm and 750 mm height drop.

**Table 4.3** Experimental Result for Impact Loading Test

Spec. No	Left Acceleration (g)		Left Displa. (mm)	Right Displa. (mm)	Maximum Strain (mm/mm)	Impact Load (kN)
	Maximum	Minimum				
3	245.26	-148.87	11.01	10.19	0.01127	10.10
4	345.21	-265.98	14.95	14.70	0.01535	13.49

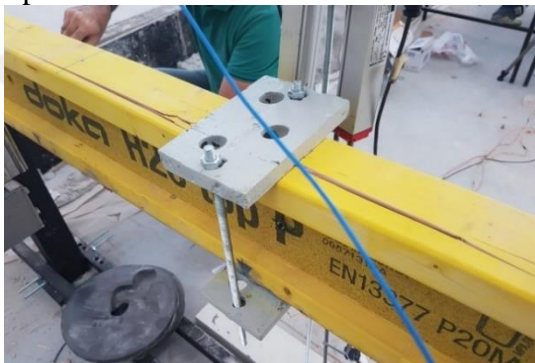
5	466.71	-307.80	20.56	20.42	0.02004	18.91
8	197.55	-127.57	9.26	9.16	0.00951	10.08
9	278.76	-167.14	12.39	12.29	0.01297	13.48
10	373.47	-264.68	17.02	16.87	0.01699	18.94



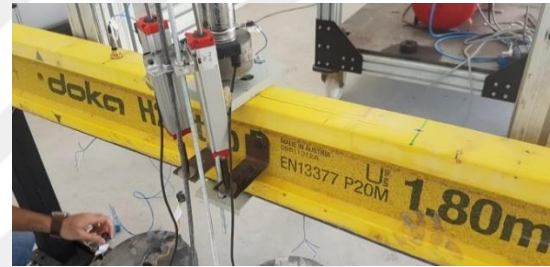
Specimen-1



Specimen-2



Specimen-3



Specimen-4



Specimen-5



Specimen-6



Specimen-7



Specimen-8



Specimen-9



Specimen-10

**Figure 4.11** Failure Modes of All Specimens



## **CHAPTER 5**

### **CONCLUSION**

Within the scope of this thesis study, general behavior and performances of CFRP fan type anchored CFRP strips and retrofitted timber formwork beams under the influence of different loading types were examined experimentally. Firstly, precast beams were damaged by loading up to a high load level of 85% of their maximum static carrying capacity. Afterwards, damaged timber beams were retrofitted with CFRP strips bonded to the bottom tension surfaces and their general behaviors and performances were interpreted by testing beams that were retrofitted under the effect of 3 different loading types until they failed. The variables examined within the scope of the experimental study are the spans of the timber formwork beams and the loading types applied to the test specimens. In this study, ‘I’ section H20 top P type timber formwork beam of DOKA<sup>®</sup> company, which is widely preferred and manufactured formwork beam as a fabricated form, has been selected as a test specimen. Tests were applied with monotonic increased static loading, high load level fatigue loading and impact loading at 3 different energy levels to the beams with 2 different spans. As a result of the tests, the load-displacement behaviors, carrying capacity, stiffness, displacement ductility ratios, energy dissipation capacities, acceleration, variation of displacement and strain values over time and the failure mechanism of the damaged retrofitted timber formwork beam test specimens under the effect of 3 different loading types are examined and interpreted. The results of the study are listed below and presented.

- Timber formwork beams are the basic formwork system components that can be influenced by many different loading types during their lifetime and they are widely used in formwork systems and carry the loads of the structure until they gain strength during the manufacturing of reinforced concrete structures. It is possible to be damaged due to various reasons and to reduce the carrying capacity during these usage periods. In the literature review, there is no comprehensive experimental study on investigating their performance under different loading types and the structural behavior of the damaged timber formwork beams produced as a

fabricated has been found. Therefore, an experimental study was conducted. It is thought that the data obtained from the study will make significant contributions to the literature on this subject. Damaged retrofitted timber formwork beams are structural elements that can be influenced by various load types such as monotonically increased static loading, high load level fatigue and impact loading during their lifetime. Behavior under these three different loading effects were examined experimentally and load-displacement behaviors were obtained. In addition, comments were made about how successful CFRP fan-type anchored CFRP strips were used as the recommended repair technique in the study.

- The recommended retrofit technique improved the performance of damaged timber beams in 3 loading types and gave successful results. The retrofit technique achieved successful performance the behavior of the retrofitted beams and had succeeded in performing 3 different loading effects although the retrofitted beams then enabled them to perform successfully in 3 different loading effects by improving the retrofit technique applied as well.
- In the proposed retrofit technique, the strips are attached to the timber beams using CFRP fan-type anchors to prevent the strips from the surface of CFRP bonded to tension surface of the beam and to be able to use all of the axial tensile force performance of the CFRP strips. This application prevented the slipping of the CFRP strips from the surface in all three loading types and enabled the effective utilization of the axial tensile force capacities of the strips by increasing the maximum strain values measured from the CFRP strips.
- When the load-displacement behaviors of undamaged reference test specimens and damaged retrofitted Specimen 1 and Specimen 6 are compared under static loading effect, it is observed that the retrofit technique applied is quite successful for two different length test specimens. Both test specimens have reached the approximate maximum carrying capacity with undamaged reference test specimens and damaged Specimen 6 displayed more energy dissipation capacity by exhibiting a much more ductile behavior than the undamaged reference test specimens. Maximum strain values measured under the effect of static loading from the test specimens retrofitted with damaged, anchored CFRP strips were obtained on average 194% larger than the strain value of the slipping from the surface for the CFRP strips given in ACI 440 R1-17 committee report.

- Undamaged timber beam test specimens with 1800 and 2450 mm long achieved much more displacement compared to damaged retrofitted with anchored CFRP strips test specimens, resulting in much more displacement under the effect of high fatigue loading. The retrofit technique applied with anchored CFRP strips has limited mid-point displacement of the beam occurring under the influence of fatigue loading much more successfully and significantly reduced.
- Maximum strain values measured from damaged retrofitted timber beams tested under the effect of fatigue loading are obtained as 378% greater than 0.005 mm / mm surface slipping strain limit value given for CFRP strips in ACI 440 R1-17 committee report. The retrofit technique applied with anchored CFRP strips allowed the CFRP strips to carry a much higher load cycle than the undamaged reference beams, which would carry an axial tension force without slipping from the surface and effectively limited the deformations of the damaged timber beams under the fatigue loading.
- It was observed that the damaged timber beams and the damaged retrofitted timber beams were close to each other when the behavior of the timber beams under impact loading were examined and the repair technique applied on damaged beams increases their performances under the impact loading of the beams and bring them closer to the undamaged beams.
- When the maximum strain values measured by impact loading are examined, the resulting values seen as 187% average greater than 0.005 mm / mm surface slipping strain limit value given for CFRP strips in ACI 440 R1-17 committee report. This result showed that CFRP strips with the effect of sudden dynamic loading without slipping from the surface effectively carry the axial tensile stress applied in the repair technique.

## REFERENCES

- [1] Porteous, J. and Kermani, A. (2007). *Structural Timber Design*. Blackwell Publishing: Malden, USA
- [2] Khelifa, M. and Celzard, A. (2014). “Numerical analysis of flexural strengthening of timber beams reinforced with CFRP strips,” *Compos. Struct.*, **111(1)**, 393–400.
- [3] Subhani, M., Globa, A., Al-Ameri, R. and Moloney, J. (2017). “Flexural strengthening of LVL beam using CFRP,” *Constr. Build. Mater.*, **150**, 480–489.
- [4] Schober, K. and Rautenstrauch, K. (2005). “Experimental Investigations on Flexural Strengthening of Timber Structures With Cfrp,” *Proc. Int. Symp. Bond Behav. FRP Struct. (BBFS 2005)*, no. Bbfs, 457–464.
- [5] D’Ambrisi, A., Focacci, F. and Luciano, R. (2014). “Experimental investigation on flexural behavior of timber beams repaired with CFRP plates,” *Compos. Struct.*, **108(1)**, 720–728.
- [6] Li, Y., Xie, Y. and Tsai, M. (2009). “Enhancement of the flexural performance of retrofitted wood beams using CFRP composite sheets,” *Constr. Build. Mater.*, **23(1)**, 411–422.
- [7] Kim, Y. and Harries, K. (2010). “Modeling of timber beams strengthened with various CFRP composites,” *Eng. Struct.*, **32(10)**, 3225–3234.
- [8] Borri, A., Corradi, M. and Grazini, A. (2005). “A method for flexural reinforcement of old wood beams with CFRP materials,” *Compos. Part B Eng.*, **36(2)**, 143–153,.
- [9] Jansson, B. (1992). “by A THESIS SUBMITTED IN PARTIAL FULFILLMENT OF Civil Engineering,” no. April.
- [10] Leijten, A. (2001). “Impact crash and simulation of timber beams,” *Comput. Eng.*, **30**, 859–868,.
- [11] Mindess, S. and Madsen, B. (1984). “The fracture toughness of wood under impact loading,” *Icf6*, 2881–2887.
- [12] Bocchio, N., Ronca, P. and Van De Kuilen, J. (2001). “Impact Loading Tests

- on Timber Beams,” *IABSE Symp. Rep.*, **85(6)**, 19–24,.
- [13] Madhoushi, M. and Ansell, M. (2008). “Behaviour of timber connections using glued-in GFRP rods under fatigue loading. Part I: In-line beam to beam connections,” *Compos. Part B Eng.*, **39(2)**, 243–248.
- [14] Yeoh, D., Fragiacom, M. and Carradine, D. (2013). “Fatigue behaviour of timber-concrete composite connections and floor beams,” *Eng. Struct.*, **56**, 2240–2248.
- [15] Tsai, K. and Ansell, M. (1990). “The fatigue properties of wood in flexure,” *J. Mater. Sci.*, **25**, 865–878.
- [16] Balogh, J. and Atadero, R. (2013). “Fatigue Testing of Wood-Concrete Composite Beams Metropolitan State University of Denver,” no. May.
- [17] Zhou, J., Huang, D., Ni, C., Shen, Y. and Zhao, L. (2018). “Experiment on Behavior of a New Connector Used in Bamboo (Timber) Frame Structure under Cyclic Loading,” *Adv. Mater. Sci. Eng.*
- [18] Thelandersson, S. and Larsen, H. (2003). *Timber Engineering*. Wiley: London, ENGLAND
- [19] Sika Group, (2006). “Product Data Sheet: SikaWrap -230 C, Woven Carbon Fiber Fabric for Structural Strengthening,” 4–6.
- [20] Sheet, P. (2006). “Sikadur ® -330,” 1–6.
- [21] Doka, (2013). “Timber formwork beams,”
- [22] Fujikake, K., Li, B. and Soeun, S. (2010). “Impact Response of Reinforced Concrete Beam and Its Analytical Evaluation,” **135(August 2009)**, 938–950.
- [23] PCB Piezotronics, (2011). “Model 353B01 ICP Accelerometer Installation and Operating Manual,”